Ahlam Oulad Ali El Hammouchi

THE EFFECT OF SUCCINATE-SUCNR1 AXIS IN NONALCOHOLIC FATTY LIVER DISEASE:

A STUDY IN A MACROPHAGE-SPECIFIC SUCNR1 KNOCKOUT MODEL

Final degree project

Directed by Dr. Carolina Serena Perelló

Biochemistry and Molecular Biology

University Rovira i Virgili – Tarragona, Spain. June 2021.

UNIVERSITAT ROVIRA i VIRGILI

About the project…

The project is done based on the curricular practicum (i.e. External practices) carried out in the Institut d'Investigació Pere Virgili (IISPV) of Joan XXIII University Hospital of Tarragona, and was supervised by Dr. Enrique Calvo Manso and Dr. Sonia Fernández Veledo (group Diabetes and metabolic associated diseases, DIAMET).

Tarragona. June 2021.

Index

Abstract

BACKGROUND: Nonalcoholic fatty liver disease (NAFLD) is an increasingly important public health problem, affecting one quarter of the global adult population. Therefore, there is an urgent need for comprehension of the subjacent mechanisms behind NAFLD pathogenesis to develop optimal therapeutic approaches. In this sense, – succinate, a metabolite from the tricarboxylic acid cycle – has been observed to activate liver fibrosis upon binding to its receptor SUCNR1 present in hepatic stellate cells. However, little is known concerning the effect of SUCNR1 activation on other NAFLD-associated mechanisms such as steatosis and inflammation.

HYPOTHESIS: A study conducted by the DIAMET group (IISPV) hinted that SUCNR1 activation in macrophages is crucial for the resolution of inflammation in a context of obesity. Since inflammation is a main factor in NAFLD progression, activation of SUCNR1 in macrophages may be key in the pathogenesis of NAFLD.

AIM: To determine whether SUCNR1 signaling in macrophages is involved in NAFLD development and progression.

MATERIALS AND METHODS: Samples from the liver, subcutaneous adipose tissue (SAT) and visceral adipose tissue (VAT) were obtained from a total of 13 mice of study, 6 of them being flox/flox) and 7 of them Myeloid cell-specific *Sucnr1* knockout mice (LysM). The mice were fed with a choline-deficient diet for 16 weeks. Levels of relative expression (mRNA) of key genes were analyzed through RT-PCR and presence of NAFLD-associated biomarkers was detected through Western Blot. Furthermore, circulating succinate and hepatic triglyceride levels were quantified. Finally, a histological study was conducted to evaluate the progression of steatosis and steatohepatitis.

RESULTS: LysM mice showed lower-than-expected levels of inflammation and only a slight tendency towards higher endoplasmic reticulum stress and lipidic metabolism alterations. Autophagy resulted to be slightly lower. No signs of fibrosis or significant steatosis were found.

CONCLUSION: *Sucnr1* deficiency in hepatic macrophages is not relevant for the development of NAFLD.

KEYWORDS: SUCNR1, succinate, NAFLD, fibrogenesis, myeloid cells

Resumen

INTRODUCCIÓN: La enfermedad del hígado graso no alcohólico (NAFLD, por sus siglas en inglés de *Nonalcoholic fatty liver disease*) es un problema de salud pública de creciente importancia, que en la actualidad afecta a un cuarto de la población adulta global. Por ello es necesario comprender los mecanismos de su patogénesis para desarrollar tratamientos óptimos. Se ha observado que el succinato – un metabolito del ciclo de los ácidos tricarboxílicos – activa la fibrosis hepática con la unión a su receptor SUCNR1 presente en las células estelares hepáticas. No obstante, se desconoce el efecto de la activación de SUCNR1 sobre otros mecanismos asociados al NAFLD, como la esteatosis y la inflamación.

HIPÓTESIS: Un estudio llevado a cabo por el grupo DIAMET (IISPV) demostró que la activación de SUCNR1 en macrófagos es crucial para resolver la inflamación en un contexto de obesidad. El receptor SUCNR1 en macrófagos podría ser clave para su patogénesis.

OBJETIVO: Determinar si la vía de señalización de SUCNR1 en macrófagos está involucrada en el desarrollo y progreso de NAFLD.

MATERIALES Y MÉTODOS: Se obtuvieron muestras de hígado, tejido adiposo subcutáneo (SAT) y visceral (VAT) de un total de 13 ratones, 6 de los cuales eran flox/flox y 7 eran knockouts de *Sucnr1* específicos de macrófago (LysM). Los ratones siguieron una dieta deficiente en colina y rica en grasas por 16 semanas. Se analizaron los niveles de expresión relativa (ARNm) de los genes clave mediante RT-PCR, así como la presencia de los biomarcadores asociados a NAFLD mediante Western Blot. Además, se cuantificaron los niveles de succinato en suero y triglicéridos hepáticos y se realizó un estudio histológico para evaluar el estado de progresión de la esteatosis y esteatohepatitis entre los grupos.

RESULTADOS: Los órganos analizados de los ratones LysM presentaron una inflamación ligeramente mayor. A su vez, sus hígados mostraban una tendencia a mayor expresión de indicadores de estrés de retículo y alteraciones en el metabolismo lipídico, así como una ligera tendencia a presentar menor autofagia. No se observaron signos de fibrosis ni cambios significativos de esteatosis respecto a los ratones control.

CONCLUSIÓN: La deficiencia de *Sucnr1* en macrófagos hepáticos no es relevante para el desarrollo de NAFLD.

PALABRAS CLAVE: SUCNR1, succinato, NAFLD, fibrogénesis, células mieloides

Abbreviations and acronyms

A

ACC: Acyl-CoA carboxylase
AMPK: AMP-activated protein kinase
ATF6: Activating transcription factor 6
ATGL: Adipose tissue TG lipase

B

BIP: Binding immunoglobulin protein

C

Cer: Ceramides
CH: Cholesterol
CHOP: CCAAT-enhancer-binding homologous protein
chREBP: Carbohydrate-responsive element-binding protein
CMA: Chaperone-mediated autophagy
CPT1α: Carnitine palmitoyl-transferase 1 alpha

D

DAG: Diacylglycerides
DIAMET: Diabetes and metabolic associated diseases
DNL: De novo lipogenesis

E

EIF2α: Eukaryotic translational initiation factor 2 alpha
ERK: Extracellular signal-regulated kinases
ER: Endoplasmic reticulum
ERAD: Endoplasmic reticulum-associated degradation
ETC: Electron transport chain

F

FAS: Fatty acid synthase
FDA: Food and drug administration
(F)FA: (Free) fatty acids
FGF: Fibroblast growth factor
Flox-flox: Sucnr1 flox/flox

G

GABA: Gamma-Aminobutyric acid
GYS-2: Glycogen synthase 2

H

HCC: Hepatocellular carcinoma
HGF: Hepatocyte growth factor
HSC: Hepatic stellate cells
HSL: Hormone sensitive lipase

I

IFN: Interferon
IISPV: Institut d'investigació Sanitària Pere Virgili
IKK: IkB kinase
IKKb/a: Inhibitor of nuclear factor-jB kinase-b
IL (6, 1B, 12…): Interleukin (6, 1B, 12…)
IR: Insulin resistance
IRE1: Inositol-requiring enzyme 1

J

JAK: Janus kinase
JAK-STAT: Janus kinase-signal transducer and activator of transcription

K

KO: Knockouts

L

LC3B: microtubule-associated proteins 1A/1B light chain 3B
LXR: Liver X receptor
LysM: LysM-Cre *Sucnr1* $^{-/-}$

M

MAPK: Mitogen-activated protein kinase
MetS: Metabolic syndrome
MGL: Monoglyceride lipase
MPO: myeloperoxidase

N

NAFL: Nonalcoholic fatty liver (benign)
NAFLD: Nonalcoholic fatty liver disease
NASH: Nonalcoholic steatohepatitis
NF-kB: Nuclear factor kappa light-chain-enhancer of activated B cells
NIK: NF-kB inducing kinase
NK: natural kill
NKT: natural kill T

O

ORF: Open reading frame

P

P62: Ubiquitin-binding protein
PEPCK: Phosphoenolpyruvate carboxykinase
PERK: PKR-like ER kinase
PI3K: Phosphoinositide 3-kinases
PIKKα/β: Phospho-IKKα/β
PPAR-γ: Peroxisome proliferator-activated receptor gamma
PYGL: Glycogen phosphorylase, liver form

Q

R

RIDD: regulated IRE-1-dependent decay
ROS: reactive oxygen species

S

S1P: Site1 protease
S2P: Site2 protease
SAT: Subcutaneous adipose tissue
(α)SMA: (alpha) smooth muscle actine
SREBP1c: Sterol regulatory binding protein-1c
STAT: Signal transducer and activator of transcription
sXBP-1: Spliced X-box binding protein 1

T

T2DM: Type 2 diabetes mellitus
TCA: Tricarboxylic acid cycle
TG: Triglyceride
TGF-B1: Transforming growth factor beta 1
TNFα: Tumor necrosis factor alpha
TLR: Toll-like receptors

U

UCP1: Uncoupling protein 1
UPR: Unfolded protein response
URV: University Rovira i Virgili

V

VAT: Visceral adipose tissue
VEGF: Vascular endothelial growth factor.

W

X

XBP-1: X-box binding protein-1

Y

Introduction

Nonalcoholic fatty liver disease (NAFLD) is defined as the hepatic manifestation of the metabolic syndrome (MetS), characterized by the presence of fat accumulation (or steatosis) in the liver in patients who do not present excessive alcohol consumption patterns. In other terms, NAFLD implies steatosis in more than 5% of hepatocytes not attributed to any secondary causes [6]. But rather than a specific disease, NAFLD is a spectrum of liver disorders.

According to the National Institute of Diabetes and Digestive and Kidney Diseases, there are two types of NAFLD: simple fatty liver (NAFL) and nonalcoholic steatohepatitis (NASH) [7]. While the first one is a benign steatosis with little to no inflammation or cell damage, the latter is the most severe form presenting inflammation, hepatocellular ballooning (rounded hepatocyte enlargement) and fibrosis, often progressing to cirrhosis, which is the end-stage organ failure requiring liver transplantation or else progressing into hepatocellular carcinoma (HCC) [6].

The diagnosis is carried out with serological tests and imaging techniques, but the current gold standard is liver biopsy, being able to distinguish between steatosis and NASH [6].

The epidemiology of NAFLD

Global prevalence and incidence

NAFLD has been predicted to become the main cause of end-stage hepatic disease worldwide. To this date it is close to being the most common chronic hepatic pathology worldwide, with its global prevalence of approx. 25% and in the United States, as the country with its biggest presence, with a prevalence of 46% [1].

NAFLD is present in both metabolically healthy and lean individuals, but it is more frequent in obese and type 2 diabetes mellitus (T2DM) patients given the closeness of NAFLD with these MetS manifestations [15].

In view of the growing epidemics of obesity and T2DM prevalence is expected to rapidly increase for the next years. NAFLD is increasingly becoming a clinical and economic burden

worldwide, and one proof of this is the estimated number of cases in Spain, being of 10.53 million in only 2016 [55].

Clinical manifestations, risk factors and severity

NAFLD is often referred to as "the silent disease" as it is mostly asymptomatic, however some patients may present fatigue, dyspepsia, pain in the liver and even hepatosplenomegaly [15].

NAFLD is closely associated with obesity and metabolic-syndrome-associated complications such as hypertension, dyslipidemia, insulin resistance (IR), central adiposity or T2DM [10]. As observed in recent studies, certain health conditions make patients more predisposed for NAFLD development as well as an accelerated progression of the disease, such as severe insulin resistance diabetes [15]. For this reason, despite of being a high prevalence disease, only a small proportion of patients present NASH with the related higher risk of hepatic fibrosis, cirrhosis, and eventual HCC. As reported in previous studies, NAFLD is not only associated with higher risk of developing HCC but also cardiovascular diseases, mainly nephropathies and neuropathies [16-17].

Consequently, individuals suffering from simple fatty liver (NAFL or Type I NAFLD) have a life expectancy similar to the general population, while those with steatohepatitis (NASH or Type II NAFLD) present cardiovascular diseases and liver-related complications that affect their survival chances [10].

Therapeutic treatments

To the date there is no pharmacological treatment approved by the FDA for NAFLD/NASH and the only available recommendations are diet and physical exercise modifications aiming at weight loss of about 5%-7%. There are different dietetic approaches, including the Mediterranean Diet, that can be proposed as a treatment for NAFLD [5].

Most of the current research done by pharmaceutical companies aim to reduce obesity-related disturbances such as insulin resistance as the main mechanism for inhibiting NAFLD progression [54]. However, there is a lack of comprehension of NAFLD effect over hepatic drug metabolizing enzymes and transporters that makes difficult the research in this area [6].

Vitamin E intake and pioglitazone as well as other insulin sensitizers have been tried and used as therapeutic approaches [6]. An example is liraglutide, a glucose-like peptide 1 analogue,

that has been proven to have a significant effect over hepatic fibrosis after a 48-week treatment [56]. Similarly, patients with ongoing hyperlipidemia have experienced significant improvement of NASH symptoms after pioglitazone use [57]. As per patients with no T2DM or other MetS complications, vitamin E remains the go-to therapeutic option, being recommended on a weekly basis [54].

The biology of NAFLD: pathogenesis and progression

In order to develop an adequate pharmacotherapy for NAFLD, it is of vital importance to understand NAFLD pathogenesis and progression which, due to its multifactorial nature, involves multiple events at molecular level, namely inflammation, hepatic fibrosis, mitochondrial dysfunction, oxidative and endoplasmic reticulum (ER) stress.

The evolution of the disease is as observed in Fig 1: from simple steatosis to steatohepatitis (NASH), evolving to cirrhosis and cirrhosis-related complications [10].

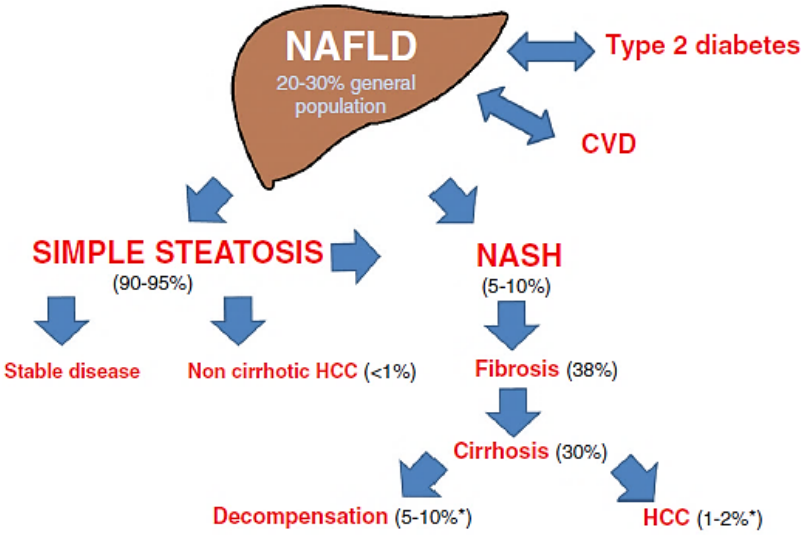

Fig. 1. Natural history of NAFLD. NAFLD is closely related to type 2 diabetes mellitus (T2DM) and obesity, two other manifestation of metabolic syndrome (MetS). The progression of the disease is as follows: healthy liver develops fat accumulation in hepatocytes (simple steatosis). At this stage, the disease is mainly stabilized, however, around 5-10% of patients progress from NAFLD to NASH, and further develop fibrosis, cirrhosis and eventually hepatocellular carcinoma (HCC). (% of prevalence/incidence), * in 10 years since cirrhosis development. Extracted from Buzzetti E et al. *The multiple-hit pathogenesis of non-alcoholic fatty liver disease (NAFLD).* Metabolism. 2016.

The mechanisms that lead to NAFLD remain unclear to this date but there have been several ones proposed, such as the role of IR in its pathogenesis [8-9], a shared key factor with T2DM.

The "two-hit" and the "multiple-hit" hypothesis

According to the initially leading hypothesis – the "two-hit" hypothesis – the lipidic accumulation in the liver is a consequence of different factors such as having a lifestyle with little to no physical exercise, following a high fat diet and having obesity. All of these factors constitute the "first hit" making the liver more sensitive to the "second hit", which is IR development, that activates pro-inflammatory signaling pathways and fibrogenesis[10].

The role of IR in NAFLD is seen in three key events: increased *de novo lipogenesis* (DNL) in the liver, up-regulation (or inhibition impairment) of lipolysis in the adipose tissue and production of pro-inflammatory adipokines and cytokines [11]. When DNL and lipolysis are increased, the result is fatty acid (FA) accumulation in the liver, in the form of triglycerides (TG). The excessive TG levels in the liver cause lipotoxicity and, in turn, mitochondrial dysfunction due to the increased reactive oxygen species (ROS) production as well as ER stress.

The development of IR has been suggested to be provoked by fatty acid modifications. The most important modification is fatty acid saturation. It has been observed that saturated fatty acids increase the phospholipid membrane's saturation, triggering unfolded protein response (UPR), ER stress and oxidative stress, all key events in the pathogenesis and progression of NAFLD [16].

Nevertheless, the "two-hit" hypothesis has been demonstrated to be too simplistic given the discovery of other factors participating in NAFLD pathogenesis, which lead to the development of a new "multiple-hit" hypothesis [10]. In addition to the effect of IR previously detailed, this hypothesis sustains that changes in the gut microbiome induce production of FA in the bowel, leading to increased permeability in the small bowel and in consequence, increased FA absorption and FA levels in blood. The higher FA blood levels contribute to the release of pro-inflammatory cytokines, such as interleukin 6 (IL6) and tumor necrosis factor alpha (TNFα) [12].

It is important to mention that some genetic variants (and epigenetic modifications) also influence the inflammatory environment of the liver, leading to a state of chronic liver

inflammation through diverse mechanisms. The consequences are the activation of hepatic stellate cells (HSC) – leading to fibrosis – and possible hepatocyte death.

In short, as observed in Fig. 2: given a combination of key factors (diet, gut microbiota, genetic factors), the patient ends up showing manifestations such as tissue damage, inflammation, fibrosis, cirrhosis and in some cases HCC.

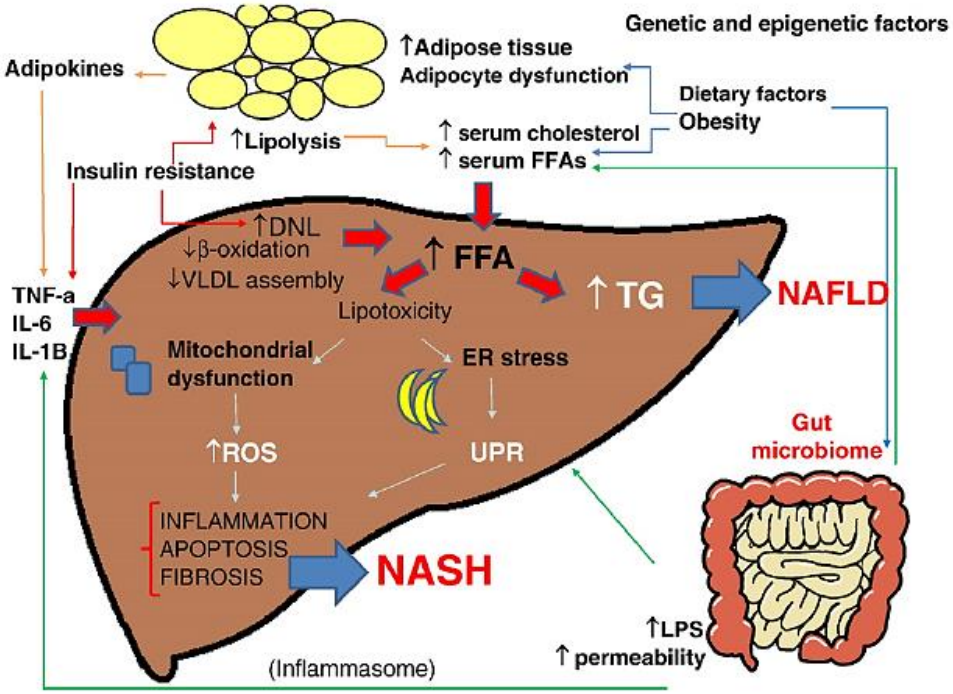

Fig. 2. Multiple hit hypothesis for NAFLD pathogenesis. Diet, lifestyle, genetics, and environmental factors raise free fatty acids (FFA) and cholesterol (CH) blood levels and induce the development of IR, adipocyte proliferation and gut microbiome changes. In the liver, IR induces DNL, increasing FFA levels, which leads to synthesis and accumulation of TG, CH and other lipids. The resulting lipotoxicity activates unfolded protein response (UPR) triggering ER stress and inflammation. Increased small bowel permeability – caused by dysbiosis – also contributes to ER stress and proinflammatory cytokine release. Finally, genetic variations also affect hepatic FA content and inflammation triggering progression into NASH. Extracted from Buzzetti E et al. *The multiple-hit pathogenesis of non-alcoholic fatty liver disease (NAFLD)*. Metabolism. 2016.

Pathogenesis and progression of NAFLD

Even though the mechanisms that explain fat accumulation in the liver have been extensively studied, the subjacent mechanisms behind the progression of the disease are not yet fully identified.

1. *From healthy liver to simple fatty liver: development of steatosis*

The first step in NAFLD pathogenesis is the accumulation of fat in the hepatic tissue, which is inherently a manifestation of MetS, also present in obesity and T2DM.

In NAFLD, fat is stored in the liver in the form of TG, which are accumulated from three different sources: intake of high-fat diets, increased lipogenesis in the adipose tissue or increased hepatic DNL.

One of the main causes of steatosis is increased adipose tissue lipolysis. As observed in Fig. 3, IR is a major contributor to steatosis as it makes the adipose tissue resistant to the effect of insulin and favors TG hydrolysis (lipolysis) into free fatty acids (FFAs) and glycerol through different enzymes, namely adipose tissue TG lipase (ATGL), hormone sensitive lipase (HSL) and monoglyceride lipase (MGL) [19]. The increased adipose tissue lipolysis leads to increased levels of FA that travel through the bloodstream to the liver where they are transformed into TG through Acyl CoA synthase activity.

Another contribution of IR to steatosis development is the upregulation of DNL. Hepatic DNL is increased trough activation of different transcription factors implicated in lipid metabolism, such as sterol regulatory binding protein-1c (SREBP1c), which is an insulin-stimulated DNL regulator, and its isoform SREBP-2c, which is involved in fat storage and the maintenance of cellular cholesterol homeostasis [18].

Other important transcription factors also implied in DNL up-regulation are: liver X receptor (LXR), an insulin-stimulated nuclear receptor that regulates cholesterol, FA and glucose homeostasis, and the carbohydrate-responsive element-binding protein (chREBP), a glucose-induced DNL stimulator [10].

2. *From steatosis to steatohepatitis: NASH development*

The progress from steatosis to steatohepatitis is the result of several mechanisms that intertwine [17]. As previously established, IR is the major driver of steatosis in NAFLD pathogenesis, but lipotoxicity and inflammation, consequence of the excessive lipid accumulation, are major drivers of NASH.

2.1. Inflammation

Inflammation is a physiological response to tissue injury, caused by lipotoxicity, ER stress and mitochondrial dysfunction as well as the activation of innate immune response, which often include cell death pathways [28].

Inflammatory pathways can be triggered by extracellular mediators, namely cytokines and lipids (eicosanoids), or by intracellular phenomena such as ER stress or mitochondrial ROS production. Some of the most important signal transduction pathways involved in NAFLD inflammation are nuclear factor kappa light-chain-enhancer of activated B cells (IKK /NF-kB) and Janus kinase-signal transducer and activator of transcription (JAK-STAT) [30].

IKK/NF-kB SIGNALING PATHWAY

The NF-kB is a major transcription factor from a highly conserved family involved in many cellular processes, mainly inflammatory responses, cellular growth, and apoptosis [29]. The NF-kB family consists of 5 structurally associated members: p50 (also NF-Kb1), p52 (also NF-kB2), RelA (also p65), RelB and c-Rel [31].

The IkB kinase (IKK) is an enzymatic complex involved in triggering the cellular response to inflammation. The IKK complex consists of two highly homologous subunits, IKKa and IKKb, and a scaffold component with no enzymatic function, IKKγ/NEMO [32]. IKK inhibits NF-kB, retaining the nuclear transcription factor to the cytoplasm.

There are two NF-kB activation pathways, the classical or canonical pathway and the alternative pathway. The first one is triggered by pathogen infection or exposure to proinflammatory cytokines that activate IKK, and its function is controlling and inhibiting programmed cell death, favoring cell survival. The latter is triggered by the TNF cytokine family, with the selective activation of IKKa by the upstream kinase NIK and is responsible for survival of premature B cells as well as development of lymphoid organs [31].

NF-kB can be activated as observed in Fig. 3. The activation of a cell surface receptor such as a Toll-like receptor (TLR), which triggers recruitment of IKK complex – often through an adaptor, e.g. TRAF [33] – leads to phosphorylation and degradation of IkB. NF-kB dimers are freed and upon their entrance to the nucleus, they regulate the transcription of multiple genes, among them those that encode proinflammatory cytokines such as IL6, growth factors, apoptotic mediators, and cell adhesion molecules [31].

As a negative feedback loop, NF-kB also up-regulates the expression of IKKa and IKKb, terminating the signaling pathway.

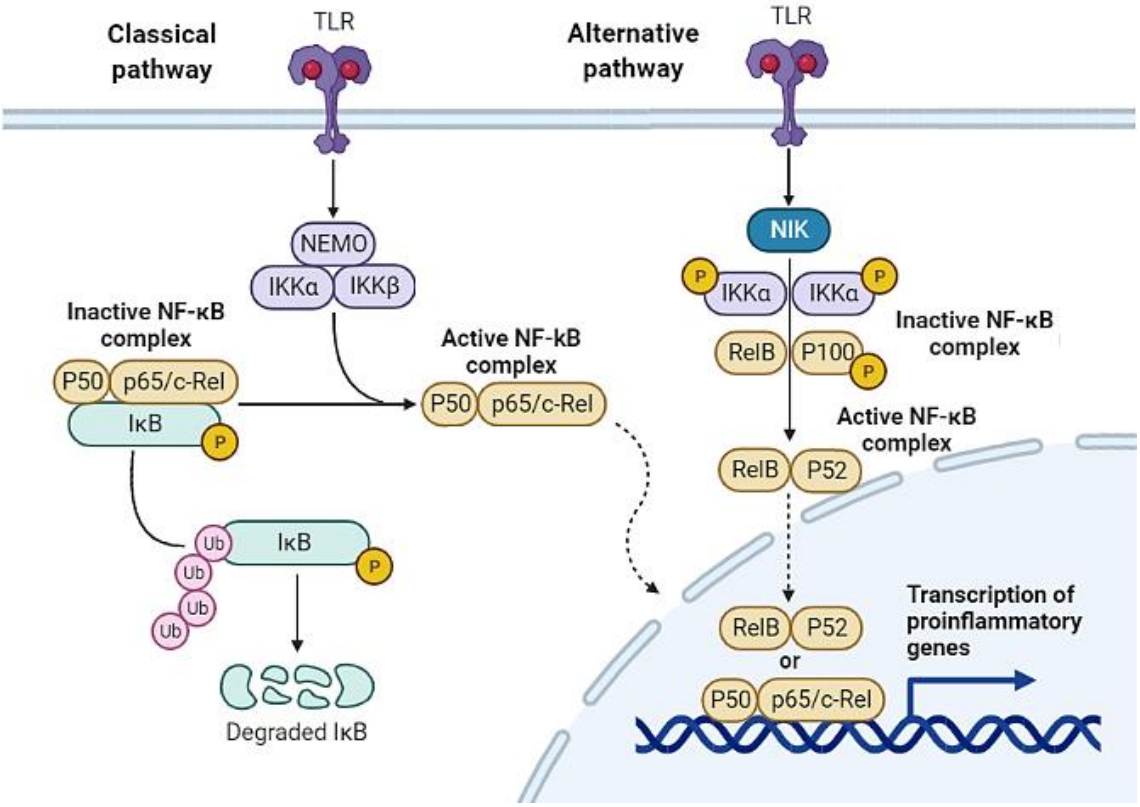

Fig. 3. IKK/NF-kB classical and alternative activation pathway. In the classical pathway, the union of a ligand to the extracellular domain or toll-like receptor (TLR) leads to activation and recruitment of the IKK complex, which is formed by three subunits: IKKa, IKKb and NEMO. Recruitment of IKK is followed by IkB phosphorylation, ubiquitination, and degradation. The classical pathway activates NF-kB dimers consisting of p50 and p65 or c-Rel. As per the alternative pathway, the IKK complex is formed of two IKKa subunits but no IKKB nor NEMO. In this scenario, upon TLR activation, the NF-kB inducing kinase (NIK) is triggered, phosphorylating the IKK complex into degradation. P100 is also degraded to p52, allowing an activated RelB/p52 complex to form. In both pathways, the active NF-kB complex travels to the nucleus to induce transcription of proinflammatory genes. Adapted from Mehcanobiology Institute 2018. *What is the NF-κB pathway?* National University of Singapore, modified via BioRender.

NF-kB is found to be active in almost every chronic liver disease (NAFLD, hepatitis, biliary liver disease). It contributes to liver homeostasis and wound-healing processes in hepatocytes, Kupffer cells and HSC. When overactivated, NF-kB triggers fibrogenesis and promotes HCC development given the chronic inflammation state of the liver.

JAK/STAT SIGNALING PATHWAY

The JAK-STAT pathway is a chain of protein interactions participating in multiple processes such as immune response, inflammation, cell division, cell death and tumor growth through the modulation of cytokines [34]. Many cytokines involved in the pathogenesis of inflammatory diseases are released through the JAK/STAT signal transduction pathway. For instance, TNFα and IL6 aggravate inflammation in rheumatoid arthritis [34].

Janus kinases (JAKs) are tyrosine kinases that form a complex with type I and type II cytokine receptors, binding to their intracytoplasmic region. JAKs contain both a catalytic domain and a second kinase-like domain with self-regulatory function. The Signal transducer and activator of transcription (STAT) proteins are a family of intracellular transcription factors that are mainly activated by membrane bound JAKs [61].

As detailed in Fig. 4, when an extracellular ligand – in this case, a cytokine – binds to the receptor, the receptor undergoes some structural changes that allow the JAKs to associate to them and phosphorylate one another. The trans-phosphorylated JAKs subsequently phosphorylate substrates that are downstream, and that includes STATs. With this phosphorylation, STATs are activated and can enter the nucleus to bind to their target genes modulating their transcription [62-63].

In mammals there are four JAK family members (JAK1, JAK2, JAK3 and tyrosine kinase2, TYK2) and seven STATs, and different ones of each are recruited depending on their tissue specificity and the receptor implicated in certain pathways [35]. Even though the classic pathway is very straight-forward, it is regulated by other signaling transductors such as the extracellular signal-regulated kinases (ERKs), mitogen-activated protein kinases (MAPK) and phosphoinositide 3-kinases (PI3Ks).

For instance, JAK1 is associated with IFN-γ, IL-6, IL-10 receptors and other receptors that share a subunit called gamma-chain, such as IL-2, IL-4, IL-7, IL-9, IL-13, IL-15 and IL-21. JAK2, on the other hand modulates hematopoietic receptors, like IL-12 and IL-23 [36].

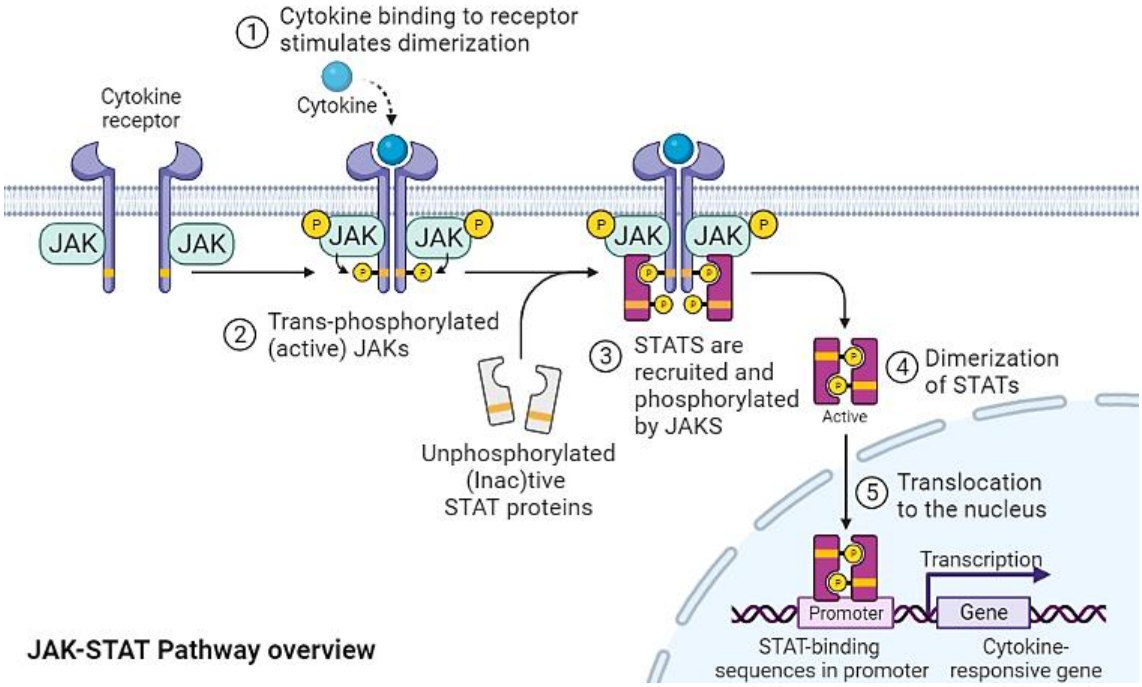

Fig. 4. An overview of cytokine signaling through JAK-STAT pathway. Upon cytokine binding to its receptor, JAKSs dimerize and phosphorylate one another. JAKs recruit and phosphorylate downstream STAT proteins, activating them. Dimerized STATs then translocate to the nucleus and regulate transcription of cytokine-responsive genes. Adapted from Abbas MN et al. *Suppressors of cytokine signaling proteins as modulators of development and innate immunity of insects*. Dev Comp Immunol [Internet]. 2020, modified via BioRender.

2.2. Mitochondrial dysfunction and oxidative stress

Lipotoxicity, consequence of steatosis, leads to several alterations in the mitochondria such as the loss of membrane polarization, making the cell unable to sustain its energetic metabolism. The damage of the beta-oxidation cycle held in the mitochondria further worsens FA accumulation, entering a vicious cycle consisting of lipotoxicity and organelle dysfunction [10].

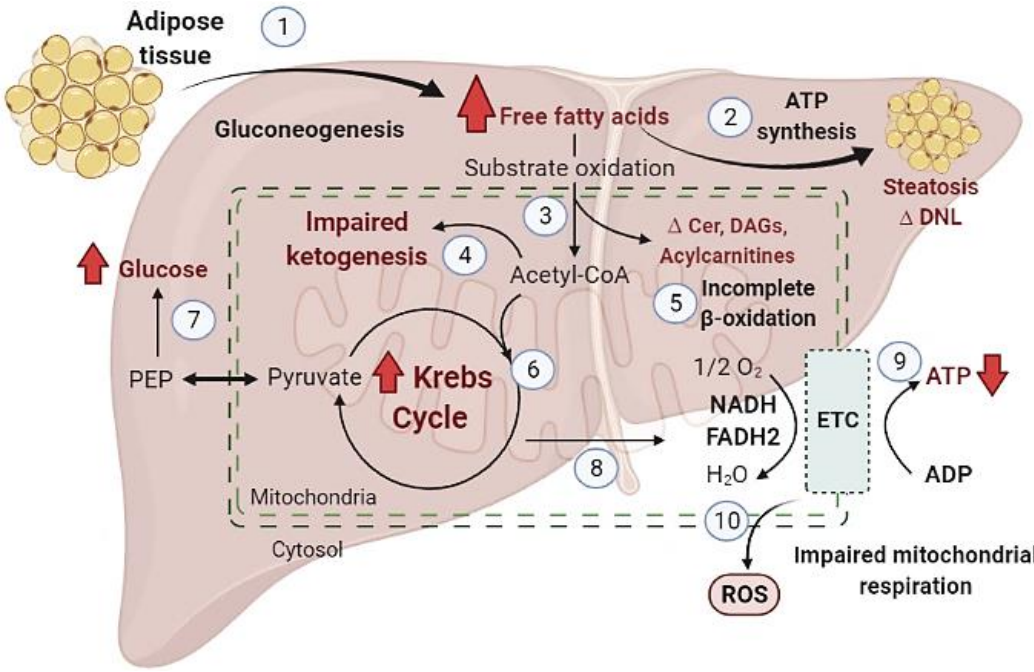

Fig. 5. Hepatic mitochondrial dysfunction during steatohepatitis development. An increased flux of FFA from the adipose tissue to the liver (1) results in accumulation (steatosis) of fat and increased DNL (2). Through beta-oxidation, FFA generate two carbon-units of acetyl-CoA (3) that are degraded through ketogenesis – nevertheless, in conditions of NASH, this pathway is impaired (4) [37]. The sum of steatosis and IR effects result in beta-oxidation losing efficiency and accumulating hepatic ceramides (Cer), diacylglycerides (DAGs) and long-chain acylcarnitines (5), while the Krebs cycle remains active (6, 7) completely oxidating acetyl-CoA to secure the energetic demands of the cell. This increased oxidative flux through the Krebs cycle during NASH has the capacity of uncoupling the Krebs cycle to the electron transport chain (ETC) (8) impairing ATP synthesis (9). Finally, the ETC impairment results in increased ROS production (10). Adapted from Sunny NE et al. *Mitochondrial Adaptation in Nonalcoholic Fatty Liver Disease: Novel Mechanisms and Treatment Strategies*. Trends Endocrinol Metab [Internet]. 2017, modified via BioRender.

As described in Fig. 5, most part of the FFA that arrives to the hepatocytes follows its normal oxidative pathway but a part of this FFA overload is destined to lipid biosynthesis of some potentially toxic intermediates, namely ceramides (Cer) and diacylglycerols (DAGs). These by-products are strong insulin signaling inhibitors in multiple inflammatory pathways, such as the c-Jun N-terminal kinase, IKK/NF-kB and TLR4 signaling pathways [69-70].

In summary, the mitochondria inability to balance the excessive lipidic storage in the liver produces impairment in the electronic transport chain (ETC) mechanism, and thus, generation of ROS in excess, which are Kupffer cell and HSC activators resulting in

fibrogenesis and inflammation, adding up to mitochondrial damage and resulting in hepatic cell death.

2.3. Endoplasmic reticulum stress

The endoplasmic reticulum (ER) is a key cellular compartment implicated in the synthesis and folding of transmembrane and secretory proteins in the cell. It is also responsible for calcium homeostasis and lipogenesis. Consequently, ER is highly involved in the pathogenesis of NAFLD. The ER in hepatocytes is a highly adaptative cellular compartment in which the protein folding process is sensitive to alterations in ER homeostasis – being susceptible to fluctuations in Ca^{2+} levels, energy, and nutrient availability – in order to ensure that vital metabolic pathways remain intact [44].

When ER homeostasis is disturbed – due to multiple factors such as activated inflammatory pathways, pathogen infections or hyperlipidemia – the entire hepatic lipid metabolism becomes dysregulated. These triggers provoke UPR activation in an attempt to restore lipidic homeostasis [38].

UPR implies activation of three signal transduction pathways through the activation of three transmembrane proteins: inositol-requiring enzyme 1 (IRE1), PKR-like ER kinase (PERK) and activating transcription factor 6 (ATF6). The aim of these signaling pathways is to attenuate ER stress via the activation of protein folding and degradation pathways.

In a first instance, these proteins remain in their inactive form united to the binding immunoglobulin protein (BIP) also named GRP78. These proteins function as ER-bond transmembrane sensors of misfolded proteins and dissociate from BIP upon activation.

ATF6 SIGNALING PATHWAY

ATF6 is present in the ER as an inactive precursor, and it consists of two domains: the intracytoplasmic domain and the surface domain – in contact with the ER lumen – that detects the presence of misfolded proteins.

Once ATF6 is activated through binding of a misfolded protein, it is released and translocated to the Golgi complex II through vesicles where it is processed and activated [44]. As observed in Fig. 6, in this compartment, ATF6 is processed by two proteins, site1 protease (S1P) and site2 protease (S2P), being cleaved in two specific sites [41].

Cleaved ATF6 is referred to as ATF6N or ATF6F [44] and its N-terminal cleaved ATF6 finally enters the nucleus where it serves as a transcription factor for UPR target genes, being chaperones such as the binding immunoglobulin protein BIP (GRP78) and GRP96, and X-box binding protein 1 (XBP-1) [42].

PERK SIGNALING PATHWAY

PERK is a kinase also consisting of a surface domain and an intracytoplasmic domain.

The external domain is bound to BIP and upon its activation it phosphorylates and activates the internal domain, in contact with the cytosol. The activated PERK phosphorylates eukaryotic translational initiation factor 2 (eIF2), turning it inactive and suppressing the initiation of translation. The aim of eIF2a inactivation is to attenuate the protein overload by holding back mRNA translation via blocking 80S ribosome assembly formation [44].

Nevertheless, inhibition of eIF2 allows for translation of some mRNA that have short open reading frames (ORF) such as ATF4 that, as seen in Fig. 6, travels to the nucleus and alters expression of genes involved in amino acid synthesis, redox processes and apoptosis [43].

ATF4 subsequentially enhances expression of transcription factor CCAAT-enhancer-binding homologous protein (CHOP) among other signal transductors involved in apoptosis. In this sense, in conditions of chronic stress PERK pathway is not protective but rather pro-apoptotic.

IRE-1 SIGNALING PATHWAY

IRE-1 consists of a surface domain that functions as a stress sensor and an intracytoplasmic domain with dual enzymatic activity: kinase and endoribonuclease activity [39].

In a similar manner to PERK, in its physiologically inactive state, the external domain is bound by the chaperone BIP [44]. As observed in Fig. 6, upon receptor activation IRE1 is freed and then phosphorylates its own internal domain.

The internal trans-phosphorylated domain becomes active and cleaves ***xbp-1*** mRNA in a nonconventional mode, with an excision of 26 nucleotides from the XBP-1 in order to generate spliced XBP-1 (sXBP-1). This spliced non-stable form of XBP-1 is a transcription factor capable of translocating to the nucleus and up-regulating target genes encoding for ER-associated degradation components, several chaperones and genes involved in lipogenesis [40].

This is the most conserved pathway among the UPR mechanisms. This pathway ultimately enhances correct protein folding and decreases the overall protein load on ER through mRNA degradation, the so-called regulated IRE-1-dependent decay (RIDD).

On a side note, enhanced RIDD can lead to pro-apoptotic signaling pathways through rapid decay of specific micro-RNAs that normally inhibit pro-apoptotic mechanisms [44].

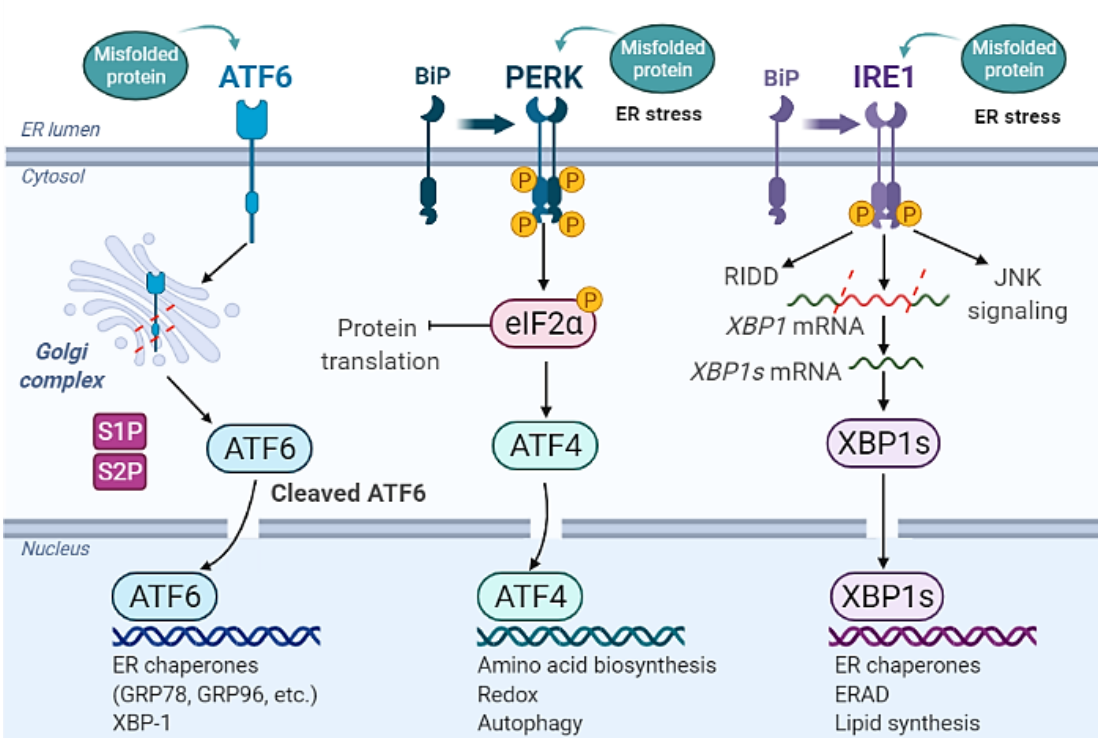

Fig. 6. Overview of unfolded protein response mechanisms. The buildup of misfolded or unfolded proteins as a consequence of ER stress leads to activation of three receptors that combined form the unfolded protein response (UPR): ATF6, PERK and IRE1. Upon activation, ATF6 is freed and transported to the Golgi complex via vesicle trafficking where it is cleaved through S1P and S2P activity generating cleaved ATF6, an activated transcription factor that upregulates ER chaperone and XBP-1 transcription. When active, PERK is freed from BIP, following a trans-phosphorylation of the cytosolic domain. The now active internal domain inhibits protein translation through eIF2a phosphorylation, except for mRNAs with short ORF such as ATF4, a nuclear transcription factor that modulates expression of genes implicated in amino acid biosynthesis, redox and apoptotic processes. In a similar manner, IRE1 is freed from BIP upon activation, phosphorylating its internal domain that has kinase and ribonuclease activity. This domain cleaves XBP-1 mRNA generating s-XBP1, a transcription factor that travels to the nucleus and regulates expression of ER chaperones, ER-associated degradation (ERAD) components and genes involved in lipid synthesis. Adapted from Jain BP. *An Overview of Unfolded Protein Response Signaling and Its Role in Cancer*. Cancer Biother Radiopharm. 2017, modified via BioRender.

2.4. Autophagy

Autophagy is a highly conserved cellular mechanism consisting of catabolic pathways for selective cellular components degradation and recycling through lysosomal activity. Autophagy has an important role in the maintenance of cellular homeostasis [48]. As observed in Fig. 7, the autophagic mechanism in mammals includes three processes: macroautophagy, microautophagy and chaperone-mediated autophagy (CMA).

MACROAUTOPHAGY

In this process a double-membrane vacuole encapsulates cytoplasm, lipid droplets and, selectively, some organelles, and proteins [48]. The procedure for selective autophagy is mediated by adaptors, such as SQSTM1/p62, which target the specific cargo through ubiquitin-mediated or ubiquitin-independent pathways [49].

CHAPERONE-MEDIATED AUTOPHAGY

This autophagic pathway is involved in the degradation of about 30% of the intracytoplasmic proteins, those containing a KFERQ motif. These proteins are detected by the chaperone Hsc70 [51] and translocated to the lysosome for their degradation.

MICROAUTOPHAGY

Microautophagy is essentially a catabolic mechanism for direct cytoplasmic components degradation. The mechanism is not yet fully understood in mammals, but it has been described as the direct delivery of the cell organelles, lipids, and proteins to multivesicular bodies in a protein chaperone-dependent manner [50].

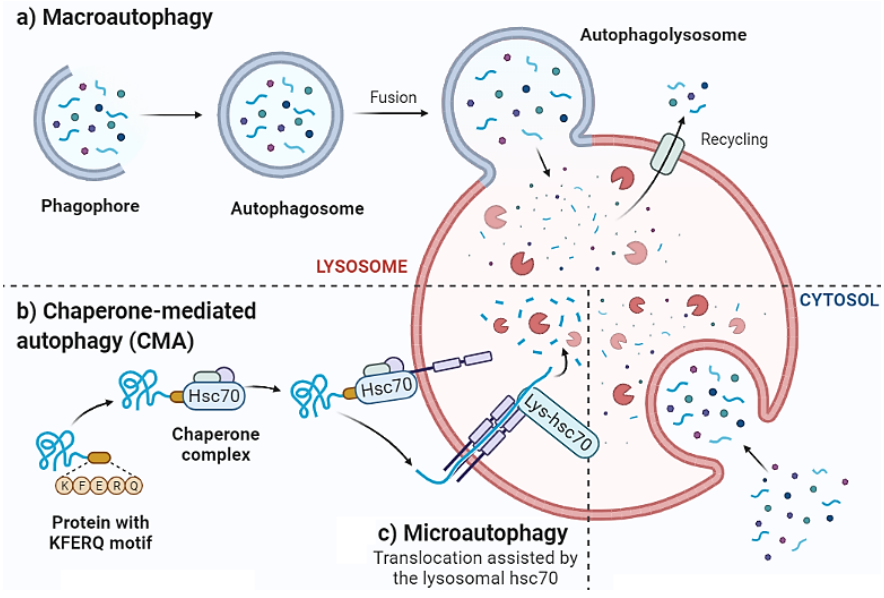

Fig. 7. Autophagic mechanisms. a) Macroautophagy is initiated with the formation of the autophagosome, which contains selective-cargo and cytoplasm-derived materials. The phagosome fuses with the lysosome, where the material is degraded and recycled. b) Chaperone-mediated autophagy (CMA) is a chaperone-mediated mechanism exclusive for proteins with KFERQ motif, which are recognized by Hsc70 chaperones, forming a complex that binds to the lysosome. c) Microautophagy is the direct delivery of cellular components from cytosol to the lysosome. Adapted from Allaire M et al. *Autophagy in liver diseases: Time for translation?* J Hepatol [Internet]. 2019, obtained from BioRender.

There is evidence suggesting that autophagy is impaired during progression of NAFLD, thus preventing elimination of the lipid excess and provoking inevitably mitochondrial damage and aggregations of toxic proteins [45].

Under NAFLD conditions, fatty hepatocytes have been observed to present a blockage of autophagosome-lysosome fusion [46], which in turn leads to protein inclusions accumulation [47]. Consequently, a vicious cycle is established where impaired autophagy aggravates steatosis, and the hepatic fat buildup further aggravates autophagy. There are four principal mechanisms for autophagic dysregulation in NAFLD:

- Decreased expression of genes encoding for autophagy-implicated proteins or decreased levels of activity of these proteins [45].
- Lysosomal basification. The increased lysosome pH, often due to a decrease in hepatic cathepsins B and L levels, implicates loss of its proteolytic activity [52].
- Blockage of autophagosome-lysosome fusion. The lipid accumulation in the hepatocyte provokes an alteration in the lipid content of autophagosomes, decreasing their capacity of fusion to lysosomes and thus impairing the autophagic pathway.

3. *The cellular response to NAFLD: histopathological consequences*

As demonstrated in previous studies, the progression of steatosis leads to histological and morphological changes in the liver: hepatocyte damage (ballooning) or death (necrosis and apoptosis), as well as HSC activation with the subsequential fibrous matrix deposition (fibrosis) [20].

Fibrosis is the result of an overactive wound healing process taking place, where connective tissue accumulates in the liver. This process is triggered in condition of chronic hepatic cell injury or inflammation and thus, the treatment implies resolving the subjacent causes.

Fibrosis starts with activation of HSC, that proliferate and start mass producing extracellular matrix components such as type I collagen. Active HSC will gradually replace hepatocytes with connective tissue in an attempt to heal the wounds [64].

In first instance fibrosis causes no symptoms to the patient, but often progresses disrupting the hepatic tissue structure and function and can lead to cirrhosis and HCC [62].

As the key prognostic marker of NAFLD, fibrosis is often used to risk stratify all patients, based on the presence and significance of fibrosis in the liver biopsy [61]. Given that non-invasive markers of fibrosis come with important limitations – poorer performance at early stages of fibrosis and with obese patients – liver biopsy remains the gold standard for NAFLD diagnose [63].

Through different tissue staining techniques, one can observe the stages of NAFLD (steatosis, inflammation, fibrosis) [20] as illustrated in Fig. 8.1 – 8. 4:

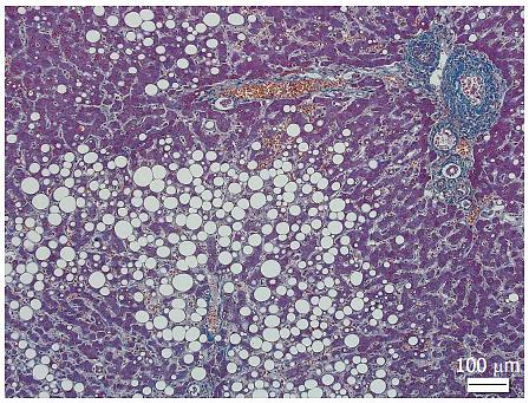

Fig. 8.1. Masson trichrome staining. Development of macrovesicular steatosis [20].

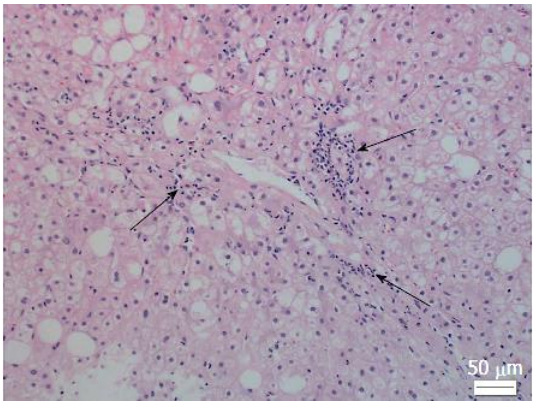

Fig. 8.2. Hematoxylin-eosin staining. Observed lobular inflammation in NASH; arrows signal necro-inflammatory foci [20].

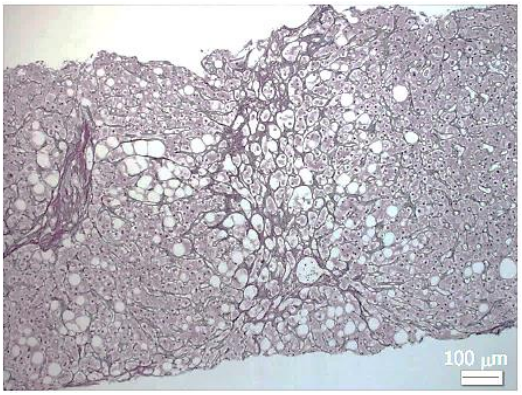

Fig. 8.3. Reticulin staining. Observable formation of pericellular fibrosis, a characteristic pattern in NASH [20].

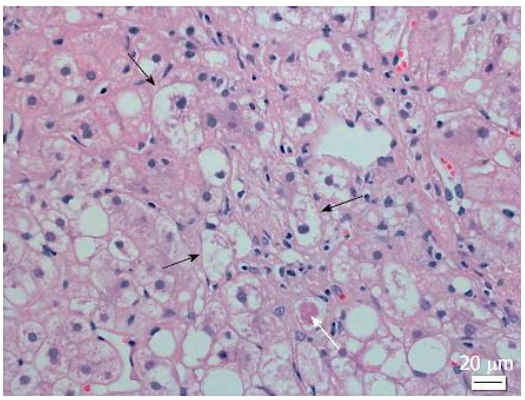

Fig. 8.4. Hematoxylin-eosin staining. Mallory-Denk bodies, aggregations of irregular eosinophiles inside the cytoplasm of the hepatocyte, signaled with white arrows [20].

All figures above (8.1 – 8.4) were extracted from Takahashi Y et al. *Histopathology of nonalcoholic fatty liver disease/nonalcoholic steatohepatitis*. World J Gastroenterol. 2014.

As mentioned earlier, HSC are the primary source of extracellular matrix components in normal and fibrotic livers [63], and thus it is essential to comprehend the mechanisms of activation of HSC in order to fully understand fibrosis.

4. *Hepatic stellate cell activation and the mechanism of fibrogenesis*

HSC (also, *ITO* cells) are resident hepatic cells found in the perisinusoidal space of the liver – the subendothelial space that represents the small area between sinusoidal endothelial cells and hepatocytes – with functions traditionally associated to retinoids (e.g. vitamin A) storage [64].

Activation of HSC essentially consists of three stages: initiation or pre-inflammatory stage, perpetuation stage and resolution stage where the liver injury finally resolves [64]:

- Initiation. The cell is triggered by paracrine stimuli (changes in the extracellular matrix and surroundings, exposure to lipid peroxides and damaged hepatocytes) and suffers changes in gene expression. The altered gene expression leads to an altered phenotype that makes the cell more responsive to other cytokines and stimuli [65].
- Perpetuation. Due to of the persistence of triggering stimuli, the altered phenotype is maintained. The activated HSC phenotype presents the following responses: proliferation, inflammatory cell infiltration, contractility, chemotaxis, fibrogenesis, matrix degradation and retinoid loss. The overall resulting effect is an enhanced accumulation of fibrous extracellular matrix, that gradually replaces normal matrix with "scar" tissue [66].
- Resolution. Certain signal transduction pathways are activated and can reverse phenotype to the quiescent form or, by contrast, drive the cell to apoptosis [67].

As observed in Fig. 9, the stimuli that trigger HSC activation are originated in the neighboring cell types, mainly sinusoidal endothelial cells, hepatocytes – damaged hepatocytes are an important source of ROS – and platelets. Kupffer cells also stimulate HSC to produce fibrous matrix and proliferate, via the release of transforming growth factor beta 1 (TGF-B1) and ROS production.

Upon activation, the HSC become highly proliferative myofibroblasts that have lost retinoid storage capacity, and their activity consists of producing different extracellular matrix components, namely type I collagen and alpha smooth muscle actine (αSMA), among others such as cellular fibronectin. As a consequence, a "pro-fibrotic" environment is established in the liver allowing for further NAFLD progression into NASH [67].

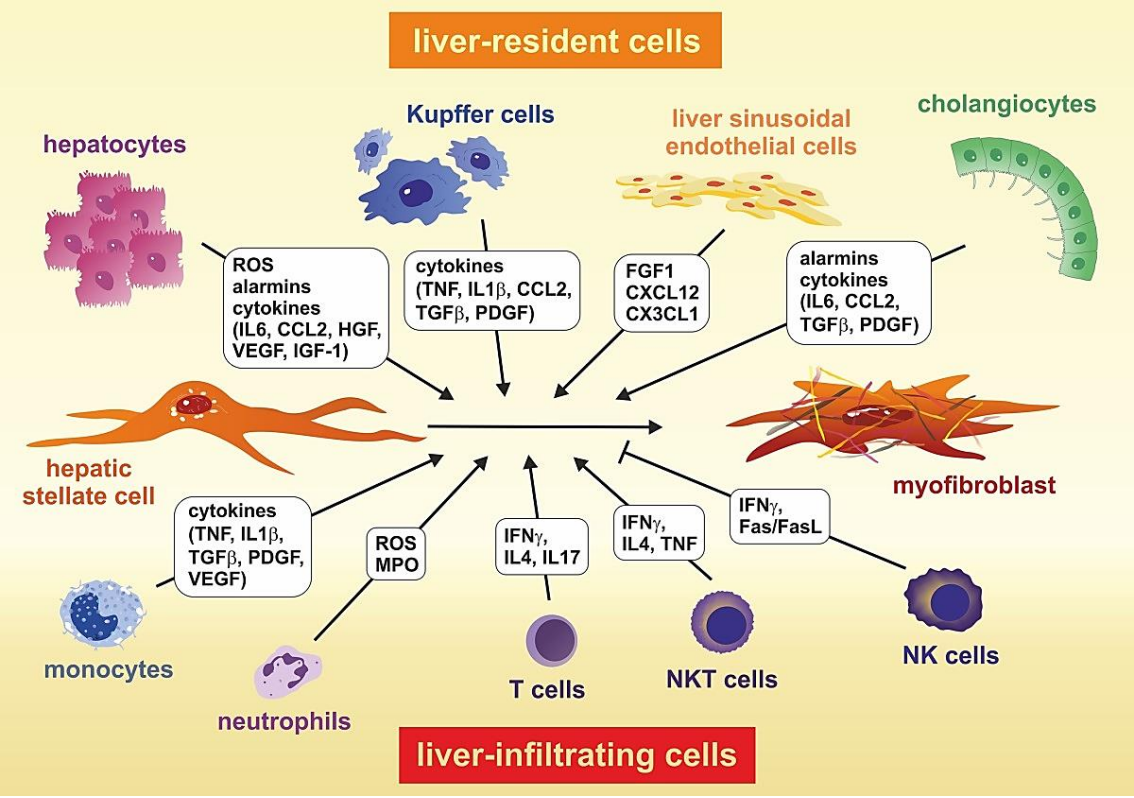

Fig. 9. Hepatic stellate cell (HSC) activation overview. The process of HSC activation is triggered by different liver-resident cell types, namely hepatocytes, monocytes, neutrophils, Kupffer cells, T cells, NKT cells, liver sinusoidal endothelial cells and cholangiocytes (biliary epithelial cells). Quiescent hepatic stellate cells undergo a transdifferentiating process to myofibroblasts. Abbreviations: FGF, fibroblast growth factor; HGF, hepatocyte growth factor; IL, interleukin; IFN, interferon; MPO, myeloperoxidase; NK, natural kill; NKT, natural kill T; ROS, reactive oxygen species; TNF, tumor necrosis factor; VEGF, vascular endothelial growth factor. Extracted from: Weiskirchen R et al. *Liver fibrosis: Which mechanisms matter?* Clin Liver Dis. 2016.

Succinate-SUCNR1 pathway and its effect on NAFLD

Succinate and SUCNR1

As conventionally defined, succinate is an intermediate metabolite of the mitochondrial tricarboxylic acid cycle (TCA) or Krebs cycle, which is synthesized in the mitochondrial matrix and participates in oxidative metabolism as a ligand in the electron transport chain (ETC) complex II. Its function is supplying electrons to the ATP synthase activity to further fuel ETC.

Nevertheless, in some specific conditions such as local stress, tissue damage or immunological activation, succinate can accumulate in the cell and diffuse into the general circulation through putative membrane transporters. In healthy humans, succinate plasma levels range from 1-50 μM and can rise mM levels in some pathological conditions such as liver damage [21-22][58].

The extra-mitochondrial/cytosolic actions of succinate are dependent on the activation of its receptor, SUCNR1 (GPR91). SUCNR1 is uniformly expressed in several metabolic tissues and its activation range 150 μM succinate levels, suggesting SUCNR1 functions as a sensor of metabolic damage rather than a physiological mediator of signaling [21].

SUCNR1 is a G protein-coupled surface receptor with a structure consisting of an alpha subunit and a beta-gamma dimer with a tight bond [59]. Upon receptor activation by succinate binding, the alpha and beta-gamma subunits dissociate, activating the MAPK pathway [60].

SUCNR1 and NAFLD development. Fibrosis and the anti-inflammatory program activated in macrophages through SUCNR1

The succinate-SUCNR1 pathway is implicated in two key processes that involve NALFD pathogenesis, which are liver fibrogenesis and inflammation.

As previously detailed, HSC is responsible for liver fibrosis development. After liver damage, activated SUCNR1 – through succinate binding – acts as a signal transductor in a pathway implicated in HSC activation. The ultimate HSC activation triggers production and accumulation of αSMA in hepatic tissue by HSC [23].

Regarding inflammation, the succinate-SUCNR1 axis has been observed to be implicated in the resolution of inflammation in a context of obesity. In obesity there is higher activation of M1 proinflammatory macrophages and lower proportion of anti-inflammatory M2 macrophages. A study conducted at the IISPV concluded that succinate-SUCNR1 signaling triggers an anti-inflammatory process which implies the switch of macrophage phenotypes from M1 to M2. The impairment of this mechanism has been identified as an inductor of the low-grade chronic inflammation observed in obesity [3].

In other terms, SUCNR1 appears to modulate macrophage phenotype polarization through secretion of type 2 cytokines (e.g. interleukin 4). It was found that a deficiency in the gene encoding for the receptor ***Sucnr1*** ultimately altered the phenotype of macrophages through inflammatory mechanisms. Consequently, *LysM-Cre Sucnr1* mice, those lacking SUCNR1 in their myeloid cells, presented local inflammation and an imbalanced glucose metabolism, as well as higher susceptibility of suffering obesity, in comparison to control mice [3].

Hypothesis and objectives

According to the multiple hit hypothesis there are several factors implicated in the progression of NAFLD. In this regard, the role of succinate might be of importance since, far from only being a simple intermediary metabolite, there is extensive evidence on succinate-SUCNR1 axis participating in liver inflammation and fibrogenesis [25-26].

Succinate-SUCNR1 axis has been observed to participate in macrophage phenotype reprograming in order to resolve inflammation under a context of obesity [3]. Since inflammation is a major event in NAFLD development, this finding allows us to hypothesize that a lack of SUCNR1 expression in macrophages would lead to enhanced inflammation in NAFLD which may trigger progression to NASH.

The final aim of the current study was to determine the role of SUCNR1 deficiency in macrophages for the pathogenesis and progression of NAFLD. For this purpose, we used samples from a murine model of C57BL/6 wild type and LysM-Cre to perform the following analyses:

- To evaluate the degree of NAFLD progression through the evaluation of steatosis, inflammation, and fibrosis.
- To analyze the alterations in liver lipid metabolism.
- To analyze ER stress and autophagy levels.

Materials and methods

Samples

To perform the study, we used samples from 13 male mice divided into two different mice genotypes:

LysM-Cre *Sucnr1* $^{-/-}$ (LysM) mice. Transgenic mice that have a myeloid-specific deletion of *Sucnr1*, n=7. These knockouts (KO) were generated by breeding with *Sucnr1* $^{flox/flox}$, the same procedure as in IISPV previous study [3].

Sucnr1 $^{flox/flox}$ (flox-flox) mice. The Cre-negative *Sucnr1* $^{flox/flox}$ mice, their *Sucnr1* allele is conditionally loxP-flanked – or "floxed". These littermates were used as controls, n=6.

The procedure to generate the LysM mice is described in Fig. 1, Supplementary material. The LysM mice had bacterial Cre recombinase activity expressed under the control of the lysozyme 2 promoter (LysMCre), this allowed for specific deletion of the *Sucnr1* gene. The genotyping of *Sucnr1* $^{flox/flox}$ mice by PCR resulted in a 450bp product for the loxP-targeted allele and a 300bp product for the wild type allele of *Sucnr1* (Fig. 2, Supplementary material).

Circulating succinate measurement

Succinate levels were quantified in serum samples of LysM and flox-flox mice with the EnzyChromTM Succinate Assay Kit (BioAssay Systems, Hayward, CA, USA), in a 96-well microplate (Thermo Scientific™, Fisher Thermo Scientific). The limit of detection was 2μM and the intra- and interassay co-efficient of variances were < 3.5 and 6.95%, respectively.

A standard curve was prepared from a succinate solution of 20mM, obtaining solutions of 0, 6, 12, 24, 40, 60 and 80μM of concentration, and the plasma samples were diluted 1/2 with H_2O. In each microwell of the plate, 20μL of each standard solution and sample was added. The following step was preparation of Working Reactive – a mix of Assay Buffer, Enzyme mix, Cosubstrate, phosphoenolpyruvate (PEP) and Dye Reagent – following the instructions of the manufacturer. On each microwell, 80μL of the Working Reactive was added, and then the plate was incubated for 30min at room temperature in the dark.

This kit is based on the transformation reaction of succinate to pyruvate, the latter being labelled with fluorescence. The fluorescent product was measured at Varioskan LUX

(Thermo Scientific™, Fisher Thermo Scientific) at 530nm, as well as 585nm in order to measure product purity through the Abs 530/585nm ratio. The standard curve served to establish a correlation between succinate concentration and absorbance through a $y=mx+b$ equation, allowing to calculate succinate concentration in the samples.

Hepatic TG levels

Tissue homogenization

The first step was homogenizing the hepatic tissue to obtain samples for FFA quantification. Approx. 10mg of tissue were isolated in Eppendorf tubes, and 200µL of 1% (w/v) Triton X-100 reagent in chloroform solution was added. The tubes were centrifuged at 13,000 x *g* for 10min. This step allowed to remove the insoluble material, and the pellet / organic phase (lower phase) was air dried at 50ºC to remove the chloroform. After this, the tubes were vacuum dried with the help of a micropipette in order to remove traces of chloroform. Finally, the dried pellet that contains the lipids was re-dissolved with 200µL of Free Fatty Acid Assay Buffer.

Triglyceride quantitative determination

Hepatic TG concentrations were measured using the Triglyceride Quantification Colorimetric/Fluorometric Kit (Sigma-Aldrich®, Missouri, USA), specifically the colorimetric method based on the reactivity of the free glycerol.

This assay is based on a reaction that generates a colorimetric product, whose absorbance is then measured through spectrophotometry. In a similar manner to the previously described quantification method, a standard curve of glycerol solutions – included in the kit – was used to obtain an equation that linked concentration to absorbance at 450nm. The concentration of the glycerol standards was expressed in terms of TG equivalents (triolein). The standard curve was established through linear regression and it was used to determine the glycerol concentration of the cuvettes that contained the samples (in triolein equivalents, CTE). The TG concentrations in the liver samples were expressed in mg per gram of hepatic tissue.

Gene expression by Real-Time PCR

Extraction of total RNA from samples

First total RNA was extracted from the sample tissues – liver, SAT and VAT – with the RNeasy Lipid Tissue Mini Kit (Qiagen Science, Hilden, Germany). Following the manufacturer instructions, approx. 100mg of tissue were homogenized with RNA TRIzol Reagent (Invitrogen Carlsbad, CA, EE. UU.). After that, 0,2mL of chloroform was added and the tubes were vortexed, followed by a centrifugation at 12000 x *g* for 10min at 4ºC. This resulted in separation of the nucleic acids – found in the aqueous upper phase – from the rest of components. This superior phase was transferred to another tube and 500µL of isopropanol was added, following another step of centrifugation at 12000 x *g* for 8min at 4ºC. The result was RNA concentrated in pellet, which was air dried and redissolved in 80µl of RNAse-free water Qiagen GmbH (Hilden, NRW, Germany). Concentration of the extracted RNA was measured through absorbance reading at NanoPhotometer ™ Implen (Munich, BY, Germany).

cDNA synthesis through RT-PCR

Of each sample of previously extracted RNA, a step of conversion to cDNA was done using the kit High-Capacity cDNA Reverse Transcription (Applied Biosystems, Foster City, California, USA). One microgram of RNA was transcribed to cDNA with random primers, the process consisted of hybridization of primer to samples (10min at 25ºC), Reverse transcription polymerase chain reaction (RT-PCR) (120min at 37ºC) and deactivation of the reverse transcriptase (5min at 85ºC). The thermocycler used was GeneAmp® PCR System 9700 (Applied Biosystems, Foster City, California, USA).

Quantitative gene expression through Real-Time PCR

Once cDNAs were obtained, they were brought to a concentration of 50ng/µL each. The 96-well microplate contained pre-defined gene assays, the TaqMan™ probes (listed in Table 2, Supplementary material). Quantitative gene expression was measured by Real-Time PCR System using TaqMan® Gene Expression Assay (Applied Biosystems, Foster City, California, USA) on a 7900HT Fast Real-Time PCR System. The software used to analyze the results was RQ Manager 1.2 de Applied Biosystems (Foster City, California, USA). The

obtained results were calculated using the comparative Ct method ($2^{-\Delta\Delta Ct}$) and the values were normalized with the housekeeping gene 18S, expressing the results as arbitrary units.

Protein expression quantification by Western Blot

Extraction of total proteins from samples

Samples of liver, SAT and VAT were homogenized in RIPA buffer – that contained Protease Inhibitor Cocktail consisting of Protease Inhibitor, Phosphatase Inhibitor, EDTA and M-PER – following the manufacturer instructions P8340 (Sigma-Aldrich®, Saint Louis, Missouri, USA). The protein concentration was measured using BCA Protein Assay Kit (Pierce Biotechnology, Massachusetts, USA).

Biomarker expression quantification through Western Blot

Following protein quantification, an equal amount of total protein of each sample was separated on SDS-PAGE gels and after running the electrophoresis, these were transferred to PVDF Immobilon® membranes (Sigma-Aldrich®, Saint Louis, Missouri, USA), and blocked for 1h at room temperature. After that an Immunoblot analysis was performed, as the membranes were incubated with the polyclonal antibodies against the markers listed in Table 1:

Table 1. Antibodies for NAFLD-associated biomarkers detection. Sources described.

Polyclonal antibody against...	
Source: Cell Signaling Technology	
Sterol regulatory element-binding protein 1c	(SREBP1c)
AMP-activated protein kinase	(AMPK)
Phospho-IKKαβ	(PIKKαβ)
Binding immunoglobulin protein	(BIP)
Eukaryotic initiation factor-2α	(EIF2α)
CCAAT-enhancer-binding homologous protein	(CHOP)
Ubiquitin-binding protein	(p62)
Microtubule-associated proteins 1A/1B light chain 3B	(LC3B)
Alpha smooth muscle actin	(αSMA)

Source: Sigma-Aldrich	
Peroxisome proliferator-activated receptor gamma	(PPARγ)
β-actin	
Source: Novus Biological	
Activating transcription factor 6	(ATF6)
Source: Santa Crux Biotechnology	
Nuclear factor of kappa light polypeptide gene enhancer in B-cells inhibitor alpha	(IKBα)
Source: Abcam	
Acetyl-CoA Carboxylase	(ACC)
Gamma-Aminobutyric acid	(GABA)
Carnitine palmitoyl-transferase I alpha	(CPT1α)

The immunoreactive bands were then visualized with SuperSignal West Femto chemiluminescent substrate (Pierce Biotechnology, Massachusetts, USA), and the captured images of the membranes were analyzed using iBright Analysis Software (Fisher Thermo Scientific).

Histopathological study

Masson's trichrome stain

This staining technique consisted in fixing the hepatic tissue samples with 4% formalin overnight, then de-hydrating them, clearing them up and finally embedding them in paraffin. This allowed to make 2µm thick sections with the microtome (Thermo Scientific, HM325). The paraffin-embedded sections were introduced in a microscope slide, incubated for 30min at 56ºC and the paraffin was cleared up with progressive cycles of Xylene and ethanol solutions. The samples were hydrated through a series of alcohol solutions (100% - 96% - 70% - 50%), being immersed for 3min each solution, and washed with distilled water for another 3min.

The samples were stained with Weigert's elastic stain first (Sigma-Aldrich, Saint Louis, Missouri, USA) for 5min and cleared up with water during 5min, followed by distilled water for 3min. The next step was Fuchsin-scarlet Biebrich staining (Sigma-Aldrich, Saint Louis, Missouri, USA) for 5min and washed up with distilled water for 2min. Then the samples

were immersed in the 5% phosphomolybdic acid solution for 2min, followed by the immersion in the 2% Light Green SF solution or fiber stain for 10min. Finally, the samples were introduced in distilled water for 3min.

After passing through the four stains, the samples were dehydrated through a scale of alcohol solutions (50% - 70% - 96% - 100%) for 30 seconds each solution and were washed thoroughly with Xylene/ethanol 1:2 solution and Xylene. In the end, the converslips were mounted with DPX mounting medium (Sigma-Aldrich, Saint Louis, Missouri, USA). The images were acquired through Leica microsystems imaging software (Wetzlar, Germany).

Statistical analysis

All values were reported as mean ± S.E.M. The obtained results were analyzed with GraphPad Prism 6.0 software. The statistical significance was determined using unpaired t-test (normal distribution) or Mann–Whitney U test (data not-normally distributed). where $p < 0,05$ values were considered as significant.

Results

Circulating succinate levels

As described in a previous study [3], succinate signaling through SUCNR1 controls an anti-inflammatory program in macrophages, inducing polarization from a proinflammatory (M1) phenotype to an anti-inflammatory (M2) one.

Levels of plasma succinate were measured in flox-flox and LysM mice, resulting in the latter having slightly higher levels as observable in Fig. 10.

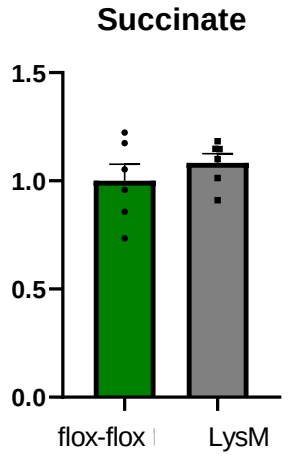

Fig. 10. Relative circulating succinate levels. Concentration of plasma succinate was measured through Succinate Assay Kit results were normalized with control group (flox-flox) mean.

Lipogenesis and lipolysis

HEPATIC TRIGLYCERIDE LEVELS

The excessive hepatic accumulation of fat – in the form of TG – is one of the major risk factors for NAFLD progression [68].

For this reason, TG levels in the liver were measured, although no significant differences were found between LysM and flox-flox as it can be seen in Fig. 11. This hints at a lack of correlation between *Sucnr1* expression in macrophages, and a tendency to accumulate fat in the liver.

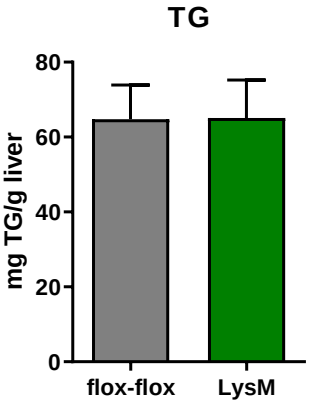

Fig. 11. Hepatic TG levels. Quantitative determination of TG levels in the liver expressed in mg of TG per gram of hepatic tissue. All values were normalized with the control group (flox-flox) mean.

HEPATIC MARKERS OF LIPOGENESIS AND LIPOLYSIS

The levels of expression of ACC, FAS, SREBP1c, PPARγ, HSL, ATGL and CPT1a in the liver were analyzed through RT-PCR. The obtained results are found in Fig. 12. LysM mice appeared to have a slightly lower than expected expression of ACC, an enzyme responsible for providing substrate (i.e. malonyl-CoA) to synthesize FA, and SREBP1c, a major regulator of fatty acids synthesis. Expression of an important regulator of mitochondrial function and hepatic fatty acid oxidation, FAS, was also lower. Similarly, genes encoding for lipases HSL and ATGL, and transporter implicated in fat oxidation, CPT1α, were also observed to be lower in LysM mice. As per PPARγ, a key factor for liver adipogenesis, the expression was much more significatively lower in comparison to controls.

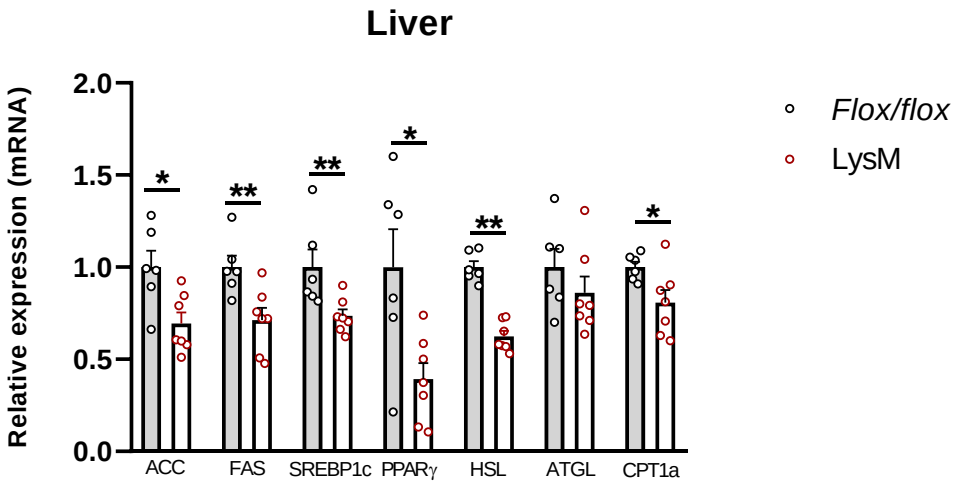

Fig. 12. Determination of relative gene expression for key genes involved in hepatic lipid metabolism. Relative gene expression of acetyl-CoA carboxylase (ACC), fatty acid synthase (FAS), sterol regulatory element-binding protein 1c (SREBP1c), peroxisome proliferator-activated receptor gamma (PPARγ), hormone sensitive lipase (HSL), adipose triglyceride lipase (ATGL) and carnitine palmitoyl-transferase 1α (CPT1α) in the liver was analyzed through RT-PCR. All values expressed as mean ± S.E.M. (n=5), with $p<0,05$.

Levels of hepatic phosphorylated AMPK (pAMPK) and ACC (pACC), PPARγ and SREBP1c were measured through Western Blot, obtaining the results of Fig. 13. The phosphorylated – and active – form of AMPK inhibits DNL activity and increases fat oxidation through phosphorylation of ACC.

In this case, both pAMPK and pACC had a lower expression in the liver of LysM mice. Similarly, SREBP1c also showed lower a slightly lower expression, whereas PPARγ levels were higher in LysM mice in comparison to controls.

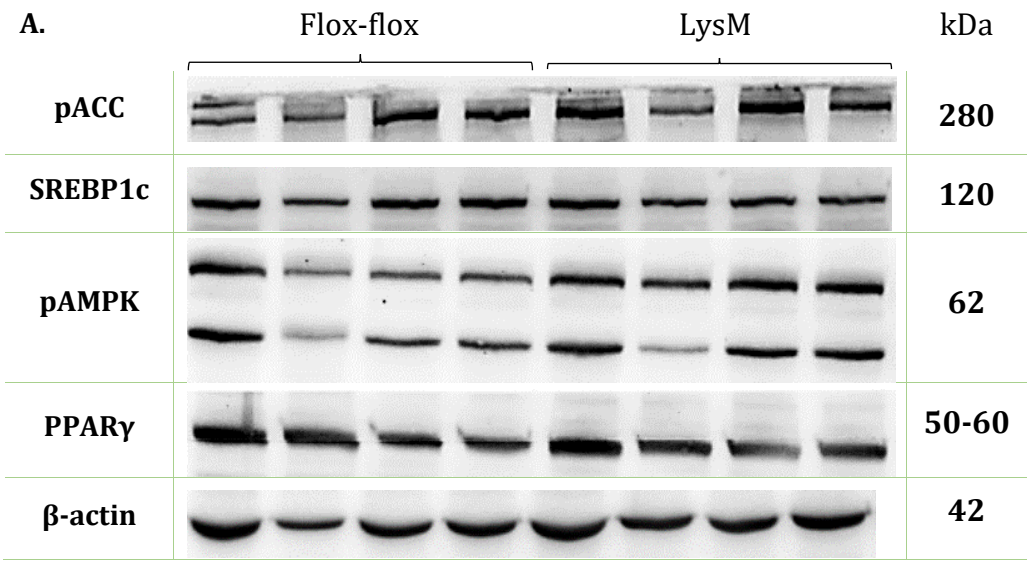

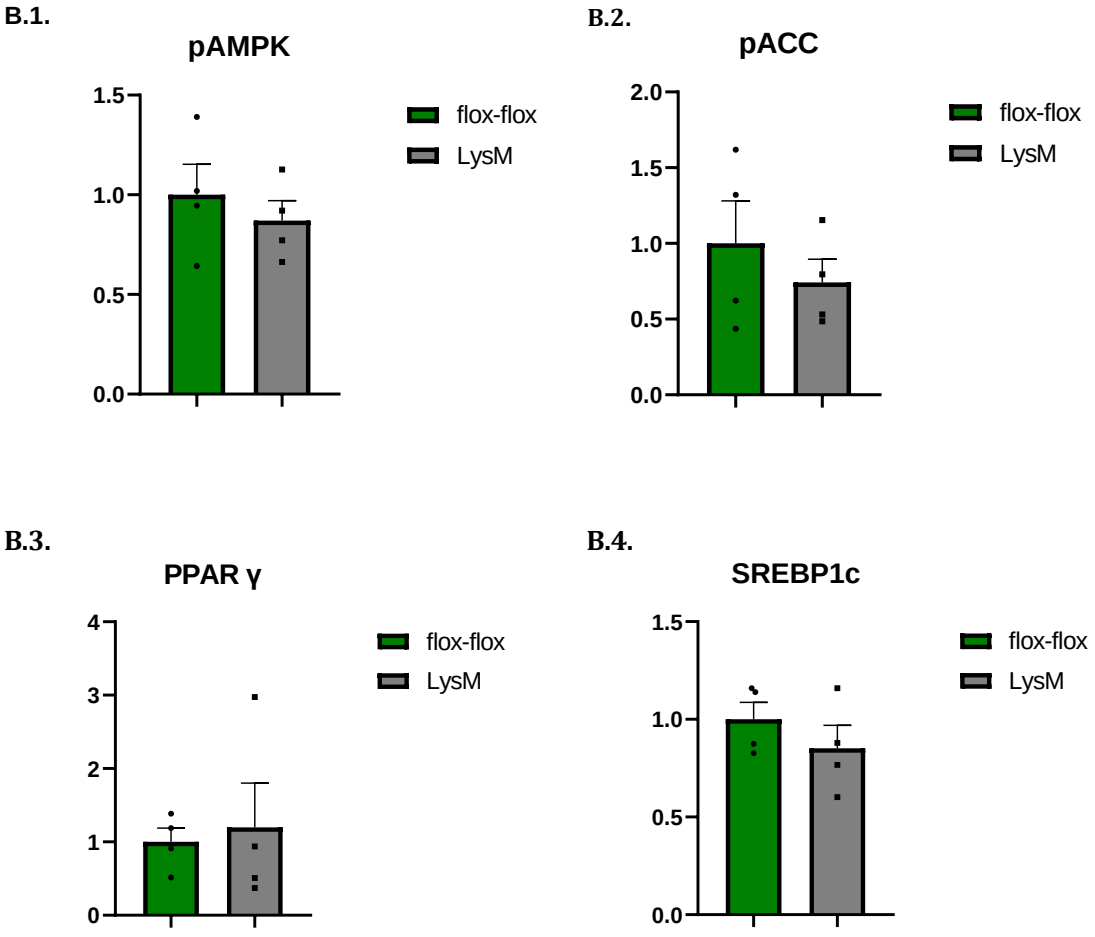

Fig. 13. Quantification of hepatic biomarkers for lipogenesis and lipolysis. (**A**) Hepatic levels of phospho- AMP-activated protein kinase (pAMPK), phospho-Acetyl-CoA carboxylase (pACC), peroxisome proliferator-activated receptor gamma (PPARγ) and sterol regulatory element-binding protein 1c (SREBP1c) obtained through Western Blot and their densitometry results (**B.1 – B.4**, respectively). All values expressed as mean ± S.E.M. (n=5), with $p<0,05$.

VAT AND SAT MARKERS OF LIPOGENESIS AND LIPOLYSIS

The relative expression of the same genes involved in lipogenesis and lipolysis was also analyzed in SAT and VAT through RT-PCR (See Fig. 14). Contrarily to the results observed in the liver, higher levels of mRNA expression of ACC, PPARγ, HSL and ATGL were observed in the VAT of LysM mice. As per the SAT, SREBP1c and CPT1α were slightly less expressed in LysM.

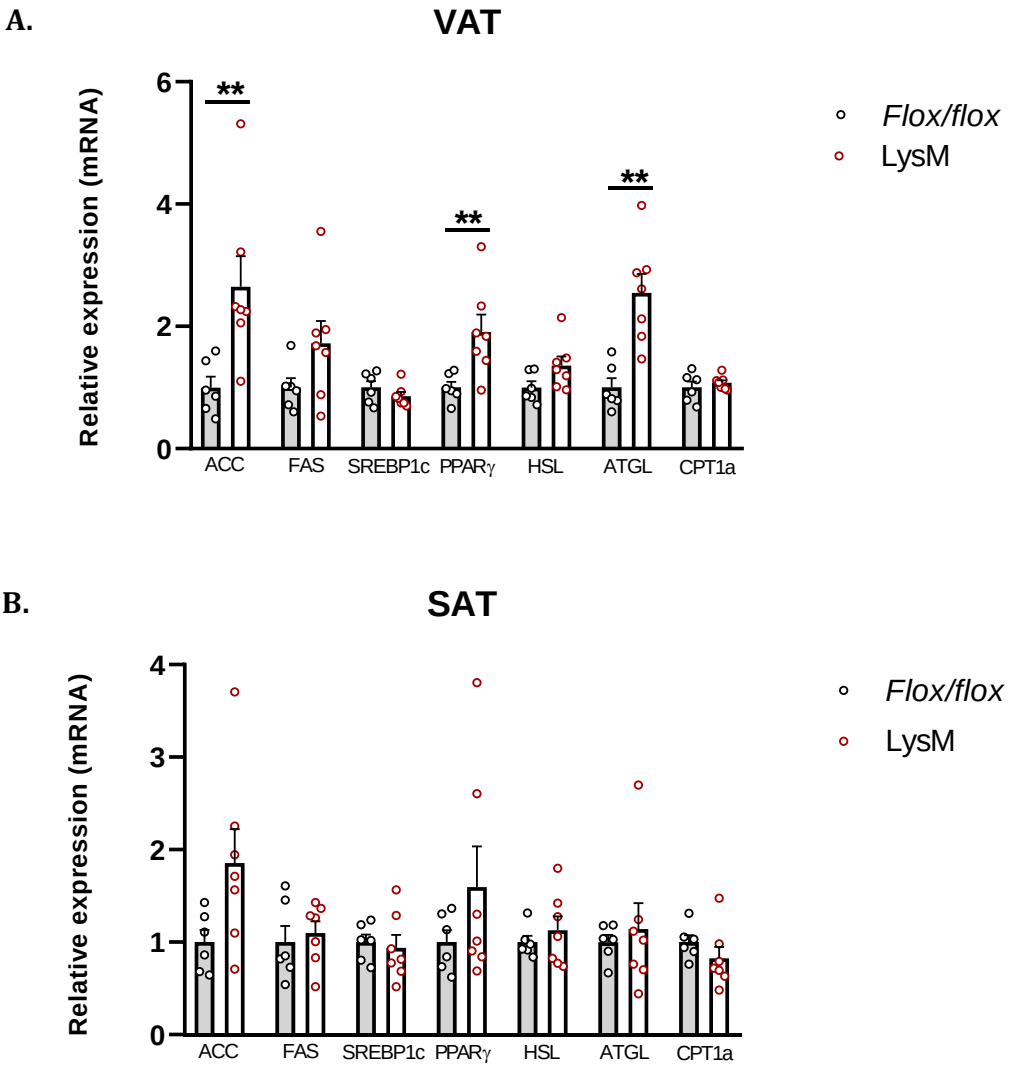

Fig. 14. Determination of relative gene expression for key genes involved in lipid metabolism in the VAT and SAT. Relative gene expression of ACC, FAS, SREBP1c, PPARγ, HSL, ATGL and CPT1α in the visceral adipose tissue (VAT) (**A**) and subcutaneous adipose tissue (SAT) (**B**) was analyzed through RT-PCR. All values expressed as mean ± S.E.M. (n=5), with $p<0,05$.

HEPATIC MARKERS OF GLYCOGEN METABOLISM

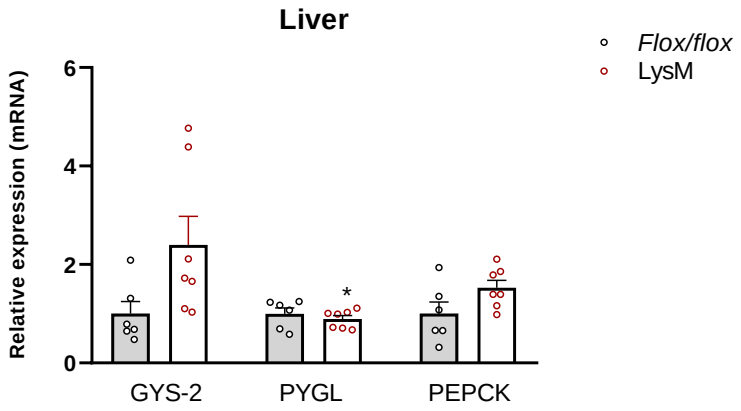

Fig. 15. Determination of relative hepatic gene expression of glycogen metabolism markers. The mRNA levels of glycogen synthase 2 (GYS-2), glycogen phosphorylase liver form (PYGL) and phosphoenolpyruvate carboxykinase (PEPCK) in the liver was analyzed through RT-PCR.All values expressed as mean ± S.E.M. (n=5), with $p<0,05$.

Relative gene expression of GYS-2 and PEPCK, two major enzymatic activities involved in glycogen synthesis and metabolism in the liver were analyzed by RT-PCR, obtaining the densitometry of Fig. 15. Both GYS-2 and PEPCK have been observed to be overly expressed in LysM mice in contrast to controls. On the other hand, PYGL, an enzyme responsible for initiation of glycogen degradation, is seen to be slightly less expressed in the liver of LysM mice.

A higher expression rate of GYS2 means enhanced glycogen synthase activity, which might signify a reduced glucose flux towards fat synthesis, repressing development of steatosis [69]. Similarly, increased levels of PEPCK implicate a higher rate of gluconeogenesis, as it is a key enzyme involved in glucose biosynthesis, which translates to reduced glucose availability for fat synthesis. In contrast, PYGL, an enzyme responsible for blood glucose homeostasis through glycogen hydrolysis, appears to be slightly less expressed in LysM. All this data combined hints at the possibility of a situation in the LysM mice liver of lower steatosis.

Inflammation

HEPATIC TISSUE

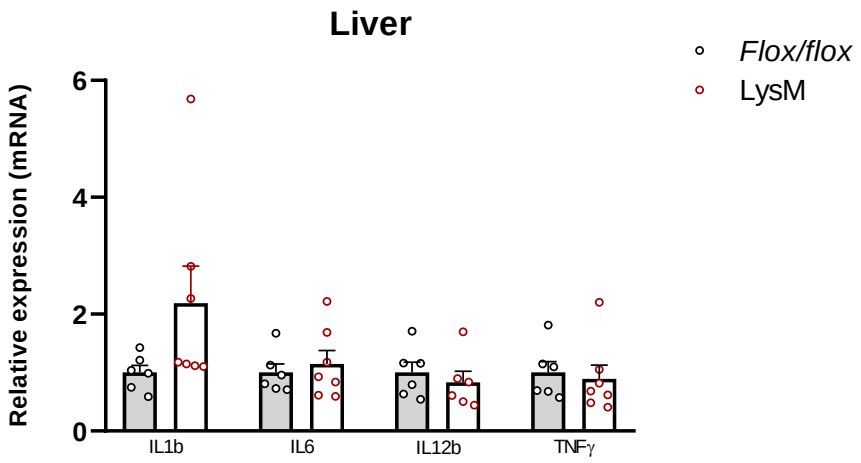

Fig. 16. Determination of relative gene expression for genes implicated in the inflammatory response in the liver. Relative gene expression of proinflammatory genes interleukin 1b (IL1b), interleukin 6 (IL6), interleukin 12b (IL12b) and tumor necrosis factor gamma (TNFγ) in the liver was analyzed through RT-PCR. All values expressed as mean ± S.E.M. (n=5), with p<0,05.

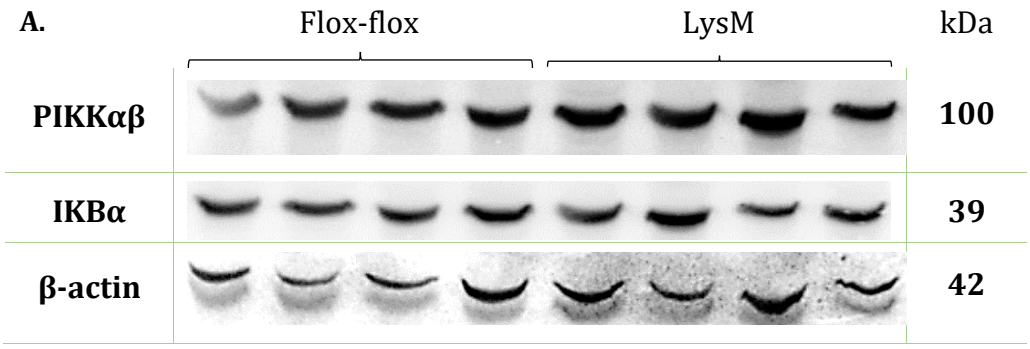

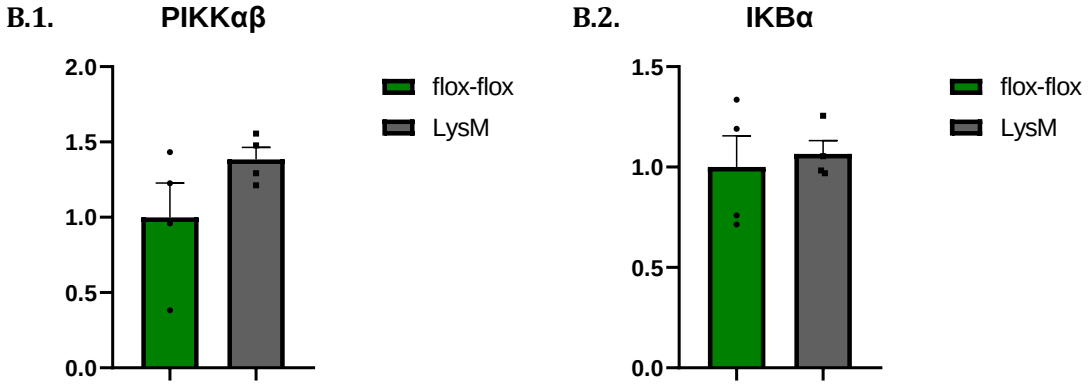

Fig. 17. Quantification of hepatic proinflammatory biomarkers PIKKαβ and IKBα. (**A**) Hepatic levels of phospho-IKKαβ (PIKKαβ) and IKBα obtained through Western Blot and their densitometry results (**B.1** and **B.2**, respectively). All values expressed as mean ± S.E.M. (n=5), with $p<0,05$.

In order to evaluate the state of inflammation of the mice, the liver, VAT and SAT were analyzed through RT-PCR and Western Blot searching for proinflammatory markers.

The results obtained from the PCR of the hepatic tissue are observed in Fig. 16. The expression of IL1b, a proinflammatory cytokine also involved in other inflammatory diseases (Chron's disease, rheumatoid arthritis), has been observed to be significantly greater in LysM mice. Nevertheless, IL1B is an exception, given that no significant differences of the other proinflammatory cytokines – IL6, IL12b and TNFγ – were found between LysM and controls.

Levels of phospho-IKKαβ (PIKKαβ) and IKBα in the liver were assessed through Western Blot. As seen in Fig. 17, LysM mice presented a slight tendency towards having more inflammation. This is seen with the increased detection of PIKKαβ and IKBα in contrast to controls.

Phospho-IKKα and IKKβ constitute the (active) catalytic subunits of IKK complex. Upon activation, IKK complex phosphorylates IKb, marking it for further degradation. The then active NF-kB complex translocates to the nucleus and induces transcription of proinflammatory genes. In this sense, PIKKαβ and IKBα serve as indication of NAFLD development due to higher activity of the proinflammatory signaling pathway NF-kB.

VISCERAL ADIPOSE TISSUE (VAT)

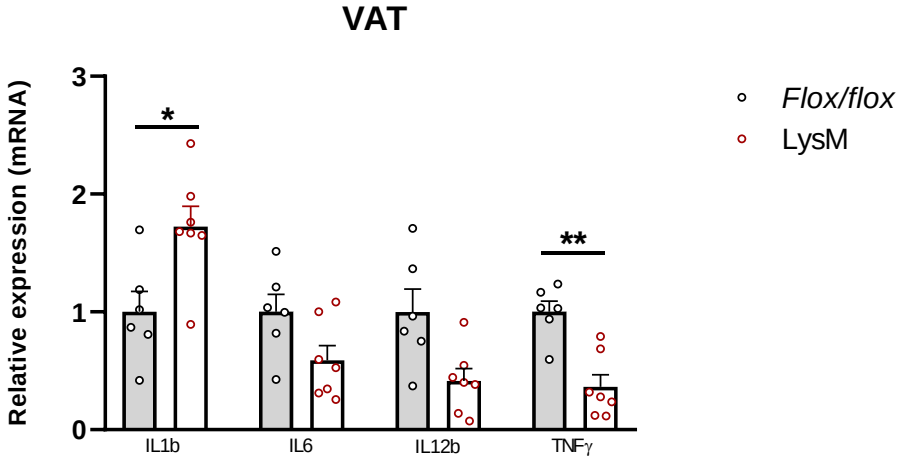

Fig. 18. Determination of relative gene expression for genes implicated in the inflammatory response in the VAT. Relative gene expression of proinflammatory genes interleukin 1b (IL1b), interleukin 6 (IL6), interleukin 12b (IL12b) and tumor necrosis factor gamma (TNFγ) in the VAT was analyzed through RT-PCR. All values expressed as mean ± S.E.M. (n=5), with p<0,05.

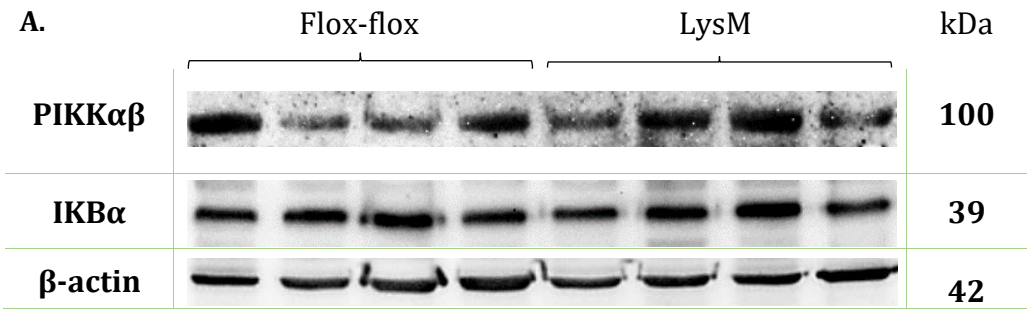

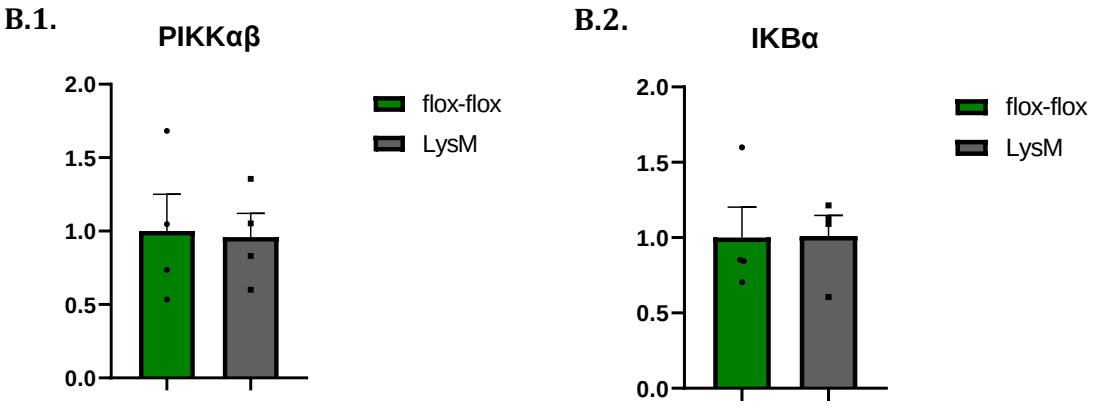

Fig. 19. Quantification of proinflammatory biomarkers PIKKαβ and IKBα in the VAT. (**A**) Levels of phospho-IKKαβ (PIKKαβ) and IKBα in the VAT obtained through Western Blot and their densitometry results (**B.1** and **B.2**, respectively). All values expressed as mean ± S.E.M. (n=5), with p<0,05.

The PCR results of the VAT, IL1B showed to be much more expressed in LysM, in contrast to IL1B, IL12B and TNFγ that had a significant decline in their expression in LysM, as observed in Fig. 18.

No significant differences between LysM and controls were found in terms of PIKKαβ and IKBα expression in VAT, as seen in the densitometries of Fig. 19.

SUBCUTANEOUS ADIPOSE TISSUE (SAT)

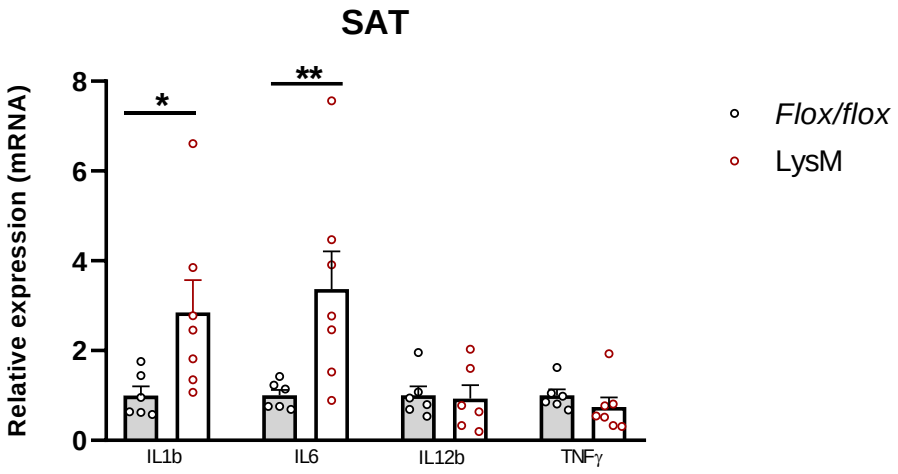

Fig. 20. Determination of relative gene expression for genes implicated in the inflammatory response in the SAT. Relative gene expression of proinflammatory genes interleukin 1b (IL1b), interleukin 6 (IL6), interleukin 12b (IL12b) and tumor necrosis factor gamma (TNFγ) in the SAT was analyzed through RT-PCR. All values expressed as mean ± S.E.M. (n=5), with p<0,05.

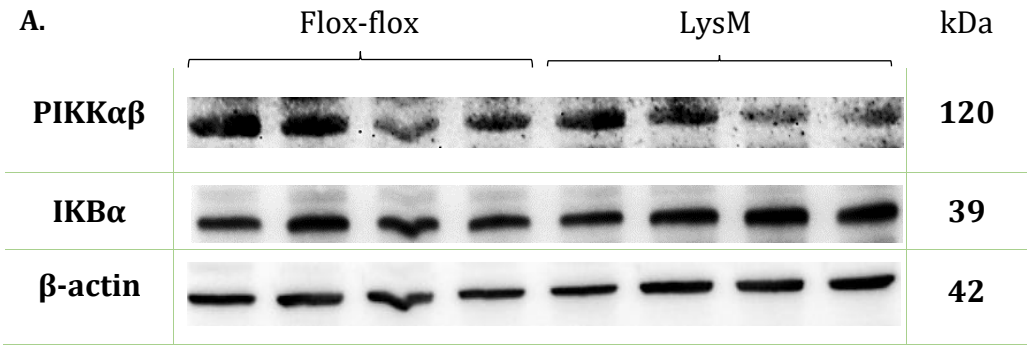

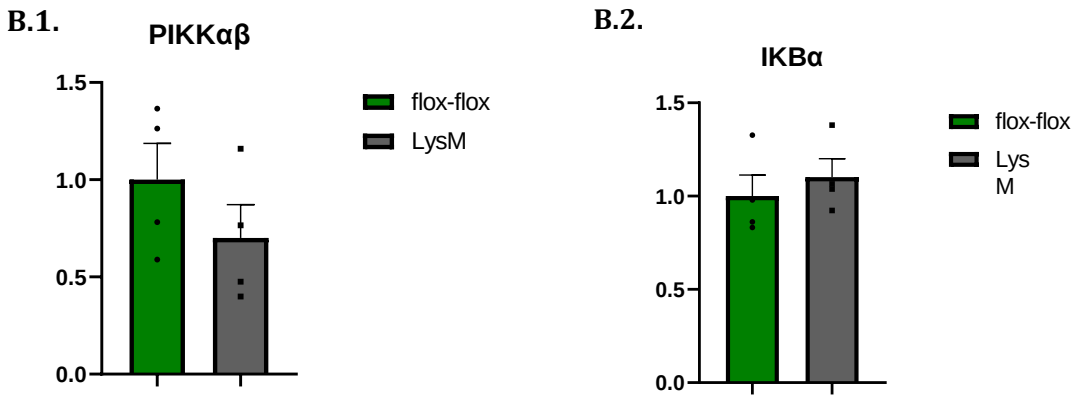

Fig. 21. Quantification of proinflammatory biomarkers PIKKαβ and IKBα in the SAT. (**A**) Levels of phospho-IKKαβ (PIKKαβ) and IKBα in the SAT obtained through Western Blot and their densitometry results (**B.1** and **B.2**, respectively). All values expressed as mean ± S.E.M. (n=5), with $p<0,05$.

The previously observed tendency in PCR results is disrupted in the samples of SAT. As observable in Fig. 20, the levels of IL6 are much higher in LysM while no significant differences between LysM and controls can be detected when it comes to IL12b and TNFγ. IL1b remains much more expressed in LysM mice.

In contradiction with the Western Blot findings in the liver, where both PIKKαβ and IKBα had higher expression in LysM, and the findings in the VAT, with no significant differences between LysM and controls, in the SAT the levels of PIKKαβ were significantly lower in LysM while levels of IKBα were slightly higher in LysM in comparison to control mice, as observed in Fig. 21.

Endoplasmic reticulum stress

HEPATIC TISSUE

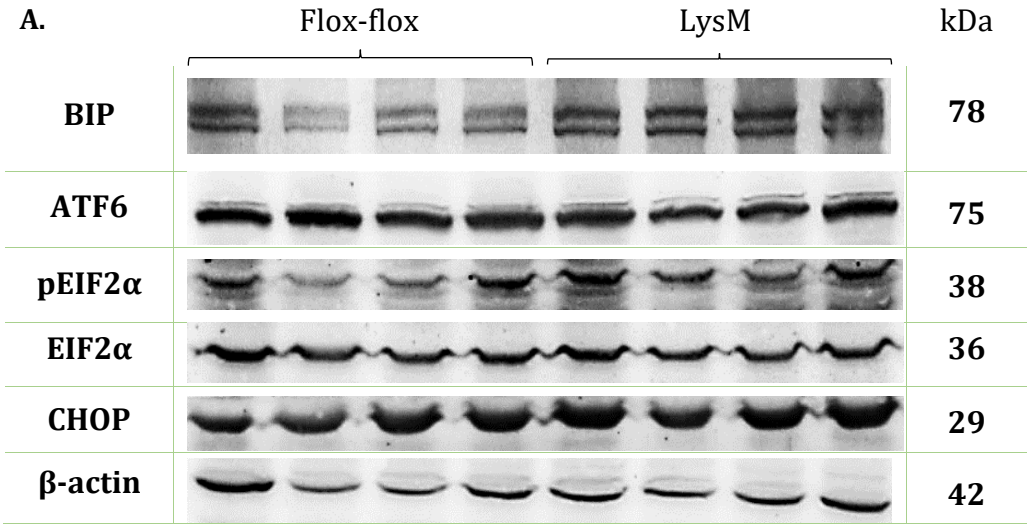

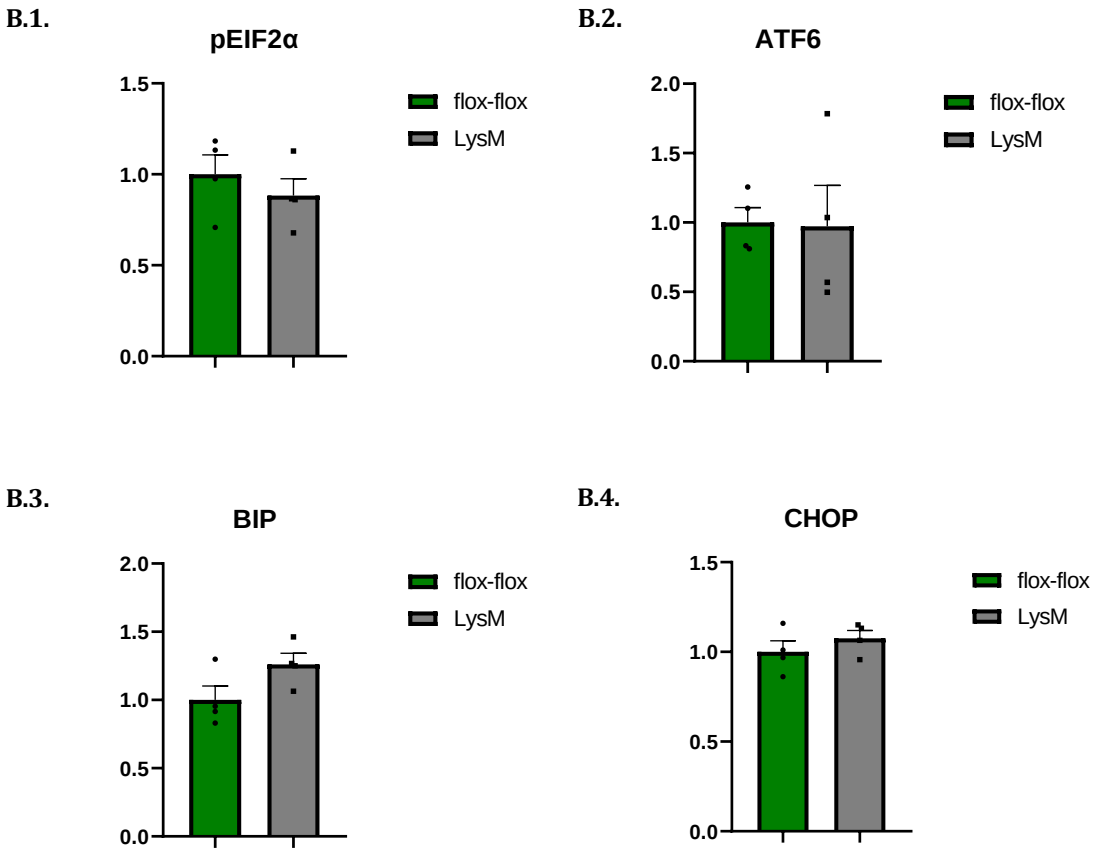

Fig. 22. Quantification of hepatic levels of ER-stress associated biomarkers. (**A**) Levels of phospho-EIF2α (pEIF2α), ATF6, BIP and CHOP in the liver obtained through Western Blot and their densitometry results (**B.1** - **B.4**, respectively). All values expressed as mean ± S.E.M. (n=5), with $p<0,05$.

Hepatic levels of pEIF2α, ATF6, BIP and CHOP were measured through Western Blot to evaluate the level of endoplasmic reticulum stress. Levels of pEIF2α and ATF6 resulted to be lower in the liver of LysM mice in contrast to controls. The eIF2α is an essential transcription factor for protein synthesis, while ATF6 is responsible for hepatic lipid metabolism homeostasis.

On the other hand, BIP, a negative regulator of UPF activation, and CHOP, a signal transductor also implicated in pro-apoptotic pathways, showed increased expression in the hepatic tissue of LysM mice, as seen in the densitometries of Fig. 22.

Autophagy

HEPATIC TISSUE

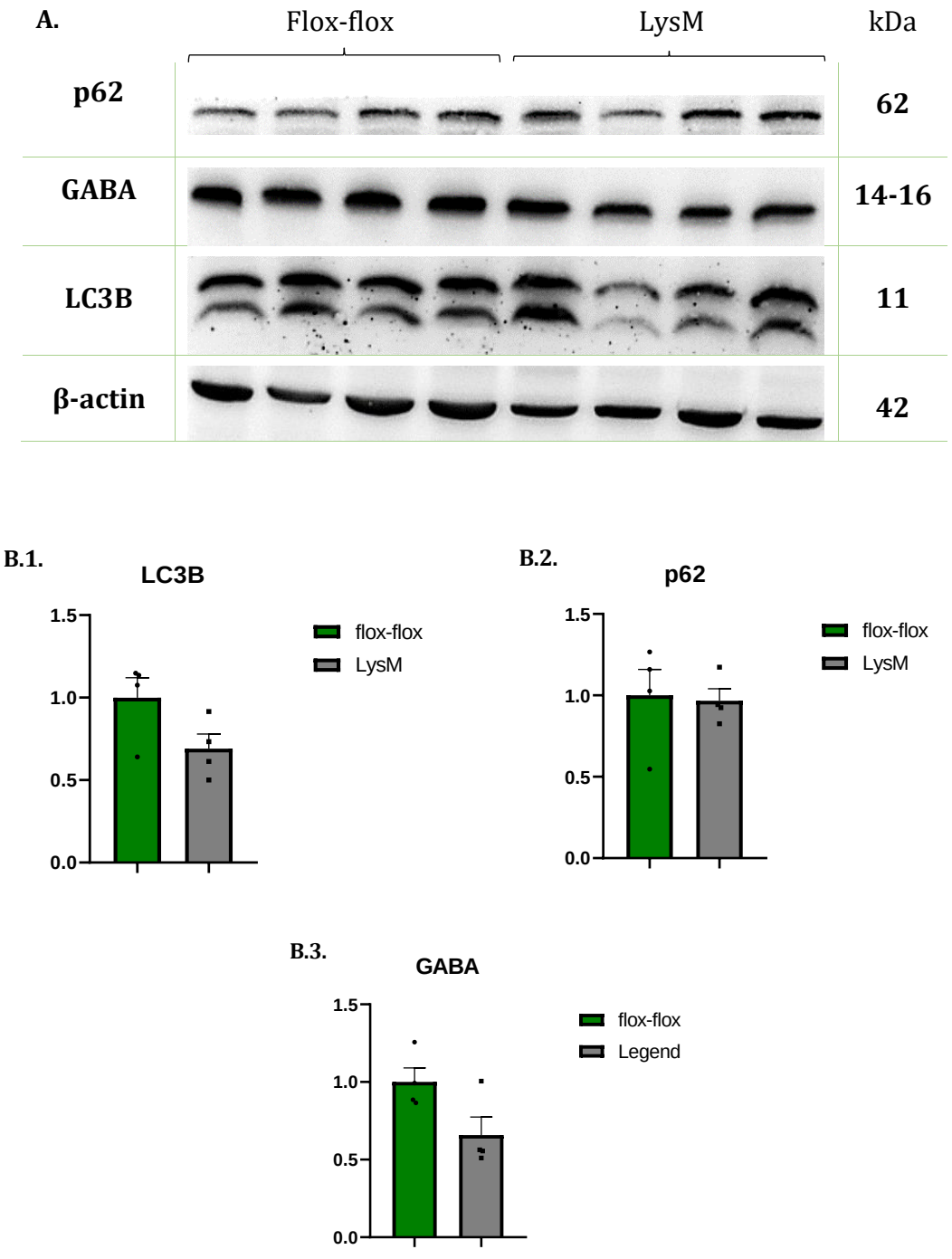

Fig. 23. Quantification of hepatic levels of biomarkers associated to autophagy. (**A**) Levels of LC3B, p62 and GABA in the liver obtained through Western Blot and their densitometry results (**B.1** - **B.3**, respectively). All values expressed as mean ± S.E.M. (n=5), with p<0,05.

The levels of three important proteins involved in autophagic transduction pathways were analyzed through Western Blot. As observed in Fig. 23, the levels of LC3B, which is a central protein in autophagy cargo selection, are much lower in LysM liver samples in comparison to controls. Similarly, levels of GABA, a neurotransmitter also implicated in improving insulin sensitivity, has been observed to be less expressed in LysM mice. Nevertheless, there were no significant differences between LysM and controls in terms of p62 expression, which is a key protein involved in the formation of hepatic inclusions with autophagy-specific substrates.

Histopathological analysis

MASSON'S TRICHROME STAIN: STEATOSIS AND FIBROSIS

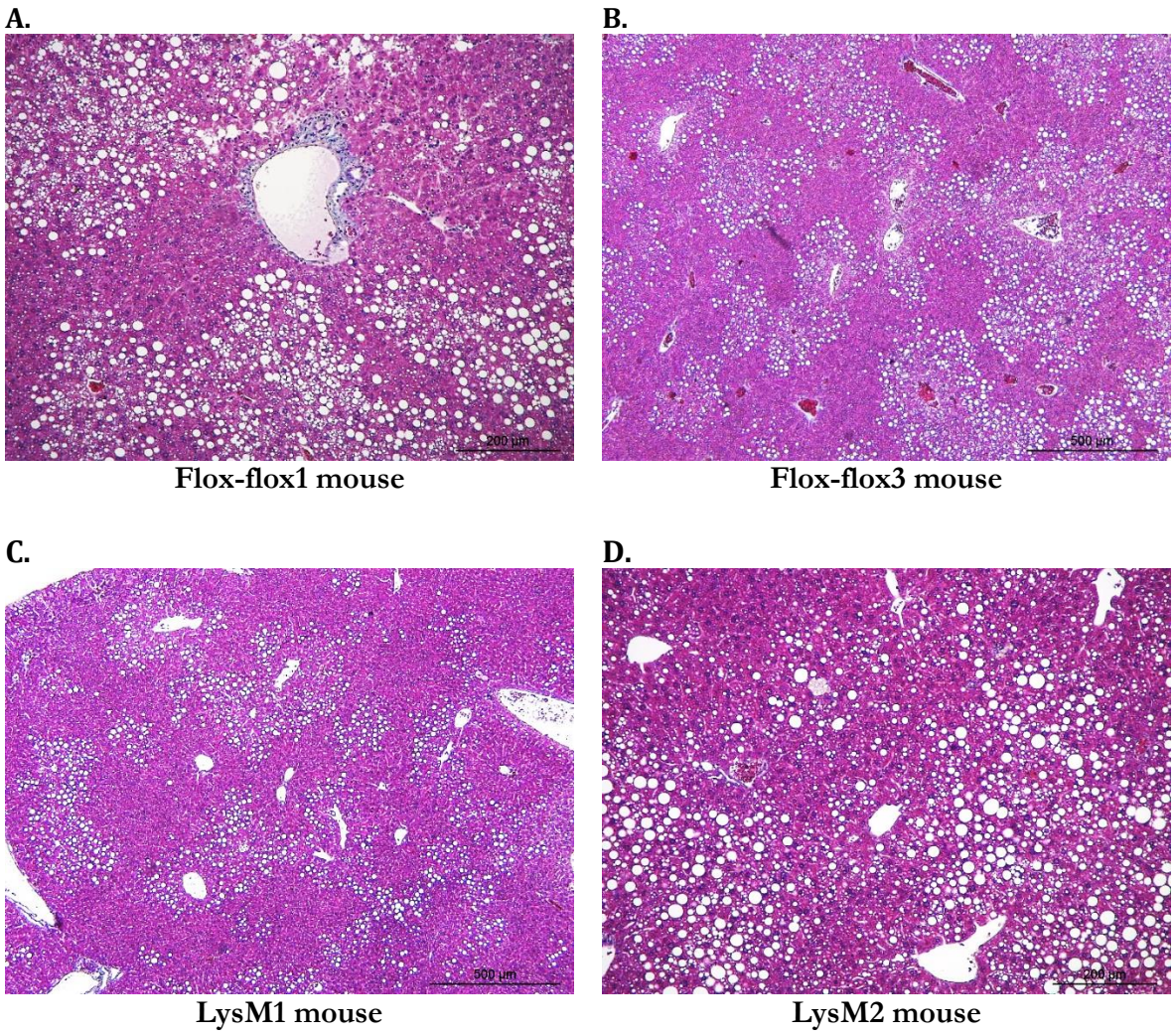

Fig. 24. Histopathological observations of flox-flox and LysM mice through Masson's trichrome stain. (**A** - **B**) Hepatic tissue of flox-flox mice and (**C** – **D**) LysM mice.

The degree of progression of NAFLD was studied through Masson's trichrome stain technique. There is no hint of liver fibrosis, and a similar degree of severe steatosis is observed in both types of mice, observed in Fig. 24.

HEPATIC TISSUE

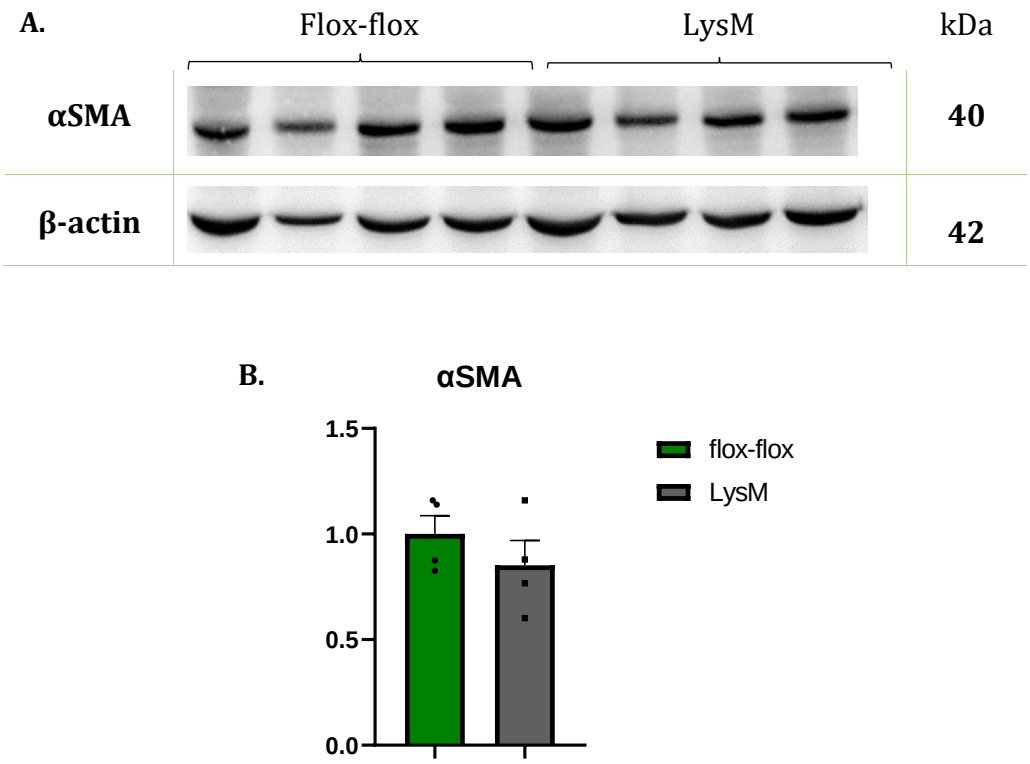

Fig. 25. Quantification of hepatic αSMA expression in the liver, through Western Blot. (**A**) Graphic representation of Western Blot results. (**B**) Quantification of αSMA expression in the liver. All values expressed as mean ± S.E.M. (n=5), with $p<0,05$.

Hepatic expression of alpha smooth muscle actin (αSMA) was measured through Western Blot, the result being a non-significant trend to lower expression of αSMA in LysM mice in comparison to controls, as clearly seen in Fig. 25.

Previous studies have demonstrated that succinate triggers αSMA production through SUCNR1 activation in HSC, for this motive it was important to evaluate αSMA levels [23].

Discussion

NAFLD has become a great burden on global health, with a prevalence exponentially rising each year due to the increasing epidemics of obesity and T2DM [13][27][53], ultimately linked to two common denominators present in modern day people lifestyles: high-fat diets and sedentary lifestyles [10]. With this rise in NAFLD cases comes a rise in awareness and in research on the topic.

In this regard, succinate, a metabolite intermediary in the TCA, is a molecule of increasing interest and a potential target for new therapies in obesity-related diseases, such as NAFLD. For instance, a relevant finding was the role of succinate receptor, SUCNR1, in hepatic fibrogenesis through activation of HSC [21]. A recent study also found that succinate-SUCNR1 axis is involved in an anti-inflammatory program in macrophages in a context of obesity. This study demonstrated that, in first instance, succinate accumulates in pro-inflammatory macrophages and is exported to the extracellular space where, due to binding to SUCNR1, a polarization of the pro-inflammatory macrophages onto an anti-inflammatory phenotype takes place [3]. This study was performed with the LysM mice, which demonstrated to be more susceptible to development of obesity, after high fat diet, than controls [3]. The current study aimed to decipher if LysM mice are also more prone to develop NAFLD.

Fat accumulation in the liver is a big risk factor for severity and progression of NAFLD [68], and as thus, the TG content in the liver was evaluated in our study. The results we found were of no significant differences between LysM and controls, which matches the findings of the hepatic levels of biomarkers associated to lipolysis and lipogenesis as well as the histopathological observations.

In the present study, contradictory results were found when assessing lipogenic, lipolytic and glycogenic markers via Western Blot and RT-PCR.

The observations we made concerning the hepatic expression of markers involved in lipid metabolism indicated an overall inferior expression of all analyzed genes – genes encoding for enzymatic activities implicated in lipolysis and transcription factors regulating lipid metabolism homeostasis – as well as inferior hepatic expression of biomarkers related to fat oxidation. These findings ultimately indicate that LysM mice have a lower rate of lipolysis and a slightly worsened IR condition, which is most certainly due to the increased DNL and the decreased presence of lipid metabolism and insulin sensitivity modulators (SREBP1c and

PPARγ). The increased DNL can be explained with the lower pAMPK and pACC hepatic levels found in LysM mice, meaning that control mice have a decreased DNL down-regulation. It is important to take into account that an augmented hepatic DNL rate is considered a cause of NAFLD development [75-77].

In contrast to the liver, the results found in VAT were of higher expression, in comparison to controls, of genes implicated in lipolysis – those encoding for lipases, transporters implicated in fat oxidation and transcription factors that regulate lipolysis – and the tendency is maintained in SAT. The conclusion of *Sucnr1* deficient mice exhibiting decreased lipolysis inhibition and increased insulin resistance is supported by an earlier study conducted on *Sucnr1* $^{-/-}$ mice where the mice were subject to a high-fat diet and the measurements of lipolytic markers revealed that the knockout mice had a lower degree of succinate-induced inhibition of lipolysis in the adipose tissue [73].

These findings hint at Sucnr1 having a role in regulation of the lipid metabolism in obesity, specifically functioning as a sensor for dietary needs and inhibiting adipose tissue lipolysis in order to maintain homeostasis.

As per glucose metabolism-associated markers, in the present study, genes involved in glycogen synthesis were analyzed in the liver and the results found that LysM had increased expression of enzymatic activities implicated in glycogen synthesis. This hints at a slight tendency of glycogenesis to function in LysM mice, as due to the increased glycogen synthesis, fat is redirected towards this pathway and not significantly accumulated in lipid droplets in the liver. This is consistent with our findings in the histopathological study of non-significative differences in steatosis manifestation.

An important factor to evaluate NAFLD progression is inflammation, given that it is a major driver of NASH and constitutes the first step into hepatic cell damage and fibrogenesis [72]. There is abundant evidence demonstrating the close link between metabolic disorders and immunity, confirming an association between obesity and a state of chronic low-level inflammation [30].

An extensive evaluation of the inflammatory state of the mice of study, LysM, was conducted through pro-inflammatory biomarker detection via Western Blot and relative mRNA expression of pro-inflammatory genes through RT-PCR: the liver, VAT and SAT were all analyzed.

Both the PCR and the Western Blot findings hinted a slight tendency towards hepatic inflammation in LysM, where the expression of IL1B, an important proinflammatory cytokine present in multiple inflammatory diseases (Chron's disease, rheumatoid arthritis, NAFLD) [81] and presence of the phosphorylated form of IKKα/β (PIKKαβ), which are the catalytic subunits that form the IKK complex, are slightly higher in the liver of LysM mice.

The IKK kinase complex is an upstream intermediary in the NF-kB proinflammatory signal transduction pathway. An increase in the active (phosphorylated) form of its subunits implicates an increased activity of this proinflammatory process taking place in the liver. Given that the obtained results for hepatic PIKKαβ expression are only almost significative because of the low number of n (samples), there must be a compensatory mechanism that resolves inflammation in the liver in the case of *Sucnr1* deficient mice. For instance, an earlier review found liver-resident macrophages (Kupffer cells) as well as infiltrated inflammatory cells – namely T cells, neutrophils, and dendritic cells – to produce IL1B in response to inflammation and steatosis, and thus it is a possibility that Kupffer cells might serve as key strategic therapeutic targets [74].

On the other hand, LysM have been observed to present increased levels of pro-inflammatory cytokine (IL1B) expression in VAT and, especially in SAT (IL1B and IL6), thus translating to a higher degree of inflammation in these adipose tissues in comparison to the results in the liver. The SAT disrupted the tendency previously observed with a clearly higher presence of inflammation as it is observable with the PCR results. Consistent with our findings, an earlier report on SUCNR1 role in obesity-induced inflammation and diabetes found that activation of SUCN1 in macrophages was crucial for inflammatory processes in adipose tissue under a context of obesity [25].

Another important factor to be studied was ER stress. Previous research showed that ER functionality could result impaired due to numerous cell alterations ultimately activating the UPR machinery [70-71]. The evaluation of ER stress-associated markers in the hepatic tissue of our study indicated a clear tendency towards ER stress in LysM mice with a lower expression of transcriptional factor pEIF2α, higher expression of BIP and no significant differences in ATF6 and CHOP expression between LysM and control mice.

The accumulation of misfolded proteins and potentially toxic metabolites in the ER triggers UPR, aiming to attenuate the ER stress through gene expression reprogramming [78]. As

previously established, UPR consists of the activation of 3 signal transducers, namely IRE1, PERK and ATF6.

During UPR activation, the translational factor EIF2α is phosphorylated turning it inactive. But pEIF2α is still capable of initiating translation of mRNA with short ORF such as ATF4. In this case, a lower hepatic expression of pEIF2α in LysM mice translates into a lower expression of ATF4, the transcription factor in charge of gene expression regulation of genes involved in amino acid synthesis, redox processes and apoptosis. This is linked to the slightly lower CHOP hepatic levels in LysM mice, as ATF4 is responsible of CHOP expression, a key intermediary in pro-apoptotic processes.

Similarly, the increased hepatic expression of BIP in LysM mice is explained through the UPR mechanism. IRE1 and PERK are initially inactive and remain bound to BIP until activated. Thus, the tendency that LysM mice showed towards ER stress in comparison to controls is explained through the partial inhibition of UPR mechanism because of BIP presence.

But as mentioned earlier, the mechanisms behind the pathogenesis and progression of NAFLD are not fully comprehended yet. This is especially obvious when it comes to ER stress, autophagy, and the relationship between these two NAFLD-associated phenomena. For instance, a study conducted around autophagy inhibition in HCC cells found that CHOP knockdown ultimately led to decreased ER stress-induced apoptosis [80].

Within a context of inflammation, altered lipid and glucose metabolism and ER-stress, autophagy is nothing but a natural point that the damaged hepatic cell often reaches. Autophagy plays a critical role in the maintenance of cellular homeostasis [45]. Our study findings also concluded with this, as LC3B, p62 and GABA were found to be less expressed in the hepatic tissue of LysM mice.

LC3B is the protein responsible for cargo selection when the autophagosome is being formed. In this sense, a lower hepatic expression of LC3B in LysM mice means overall less autophagic mechanisms. The same way, p62 was also expected to be lower as it is the receptor for cargo destined for autophagic degradation. Similarly, the lower hepatic GABA levels were logical as GABA mediates selective autophagy via binding to its autophagic receptors (e.g. p62).

In an earlier study conducted on high-fat diet fed NAFLD mice, hepatic levels of ER stress and autophagy biomarkers were analyzed, and the concluding evidence supports the findings of our study [79]. This study had taken into account the results of mice with simple steatosis (NAFL) and mice of a more progressed state of the disease (NASH) finding that the latter presented significantly higher levels of markers CHOP, p62 and LC3B.

This tendency towards lower levels of autophagy in LysM mice could hint at SUCNR1 being involved in pro-apoptotic processes.

Lastly, the histopathological study showed that no fibrosis was present and no significant differences in terms of steatosis were observed between LysM mice and controls, confirmed by evaluation of αSMA expression. It is important to highlight that the present study was conducted evaluating samples from mice that were fed a choline-deficient high-fat diet for 16 weeks and the lack of clear signs of fibrosis – of both LysM and control mice – could be consequence to the contents of the diet or the length of the period the mice of study were subjected to.

Conclusions

The expression of *Sucnr1* in hepatic macrophages appears to not have a significant relevance in terms of the pathogenesis and progression of NAFLD. As the SUCNR1-deficient mice showed a slightly higher tendency to develop inflammation, SUCNR1 is confirmed to play a role in the resolution of inflammation in the liver, although there is most certainly a compensatory mechanism for inflammation resolution in which Kupffer cells may take part, that is exhibited with the higher IL1B expression. Also, the slightly higher tendency towards ER and lower tendency toward autophagy observed in LysM mice could hint at SUCNR1 being involved in the UPR signaling machinery. On the other hand, contradictory results were found in terms of lipid metabolism and glycogen synthesis alterations, and thus it is not possible to make a concluding statement on this matter.

Acknowledgements

"No one who achieves success does so without the help of others. The wise and confident acknowledge this help with gratitude." – Alfred North Whitehead, English mathematician and philosopher.

The entirety of this project was carried out during my curricular practicum period at IISPV. It is only fair to acknowledge the many DIAMET members and doctoral candidates that have helped me with the laboratory tasks. The presence of my colleague Natalia Gallego was also very enriching for this experience, as we did a lot of teamwork and coordination of the different tasks whenever it was necessary.

I would also like to thank my mentor for guiding me during this whole experience, Dr. Enrique Calvo, whose patience allowed me to shape not only this project but also my way of understanding the life of a professional scientist and researcher. My very sincere appreciation of his hard work and implication in the elaboration of this final degree project.

Finally, a special thank you to Dr. Carolina Serena, who did a great job as a project tutor, thanks to her constant offers of help and ongoing communication with me during the back-and-forth work perfecting process.

References

1. Cotter TG, Rinella M. Nonalcoholic Fatty Liver Disease 2020: The State of the Disease. Gastroenterology [Internet]. 2020;158(7):1851-64.
2. Mantovani A, Scorletti E, Mosca A, Alisi A, Byrne CD, Targher G. Complications, morbidity and mortality of nonalcoholic fatty liver disease. Metabolism [Internet]. 2020;111:154170.
3. Keiran N, Ceperuelo-Mallafré V, Calvo E, Hernández-Alvarez MI, Ejarque M, Núñez-Roa C, et al. SUCNR1 controls an anti-inflammatory program in macrophages to regulate the metabolic response to obesity. Nat Immunol. 2019;20(5):581-92.
4. Fouad Y, Waked I, Bollipo S, Gomaa A, Ajlouni Y, Attia D. What's in a name? Renaming "NAFLD" to "MAFLD". 2020;(April):1254-61.
5. Torres MCP, Aghemo A, Lleo A, Bodini G, Furnari M, Marabotto E, et al. Mediterranean diet and NAFLD: What we know and questions that still need to be answered. Nutrients. 2019;11(12):1-19.
6. Cobbina E, Akhlaghi F. Non-alcoholic fatty liver disease (NAFLD) - pathogenesis, classification, and effect on drug metabolizing enzymes and transporters. Drug Metab Rev. 2017;49(2):197-211.
7. Diehl AM, A Tetri B. National Institute of Diabetes and Digestive and Kidney Diseases (NIDDK). National Institutes of health. 2016. Available at: https://www.niddk.nih.gov/health-information/liver-disease/nafld-nash/definition-facts
8. Chen Z, Yu R, Xiong Y, Du F, Zhu S. A vicious circle between insulin resistance and inflammation in nonalcoholic fatty liver disease. Lipids Health Dis. 2017;16(1):1-9.
9. Fujii H, Kawada N. The role of insulin resistance and diabetes in nonalcoholic fatty liver disease. Int J Mol Sci. 2020;21(11).
10. Buzzetti E, Pinzani M, Tsochatzis EA. The multiple-hit pathogenesis of non-alcoholic fatty liver disease (NAFLD). Metabolism [Internet]. 2016;65(8):1038-48.
11. Fatty N, Disease L, Treatments PN. Nonalcoholic Fatty Liver Disease and Potential New Treatments. 2017;(Figure 1):1-13.
12. Kirpich IA, Marsano LS, McClain CJ. Gut-liver axis, nutrition, and non-alcoholic fatty liver disease [Internet]. Vol. 48, Clinical Biochemistry. Elsevier B.V.; 2015. 923-930 p.
13. Lazarus J V., Colombo M, Cortez-Pinto H, Huang TTK, Miller V, Ninburg M, et al. NAFLD — sounding the alarm on a silent epidemic. Nat Rev Gastroenterol Hepatol [Internet]. 2020;17(7):377-9.
14. Milić S, Lulić D, Štimac D. Non-alcoholic fatty liver disease and obesity: Biochemical, metabolic and clinical presentations. World J Gastroenterol. 2014;20(28):9330-7.
15. Pafili K, Roden M. Nonalcoholic fatty liver disease (NAFLD) from pathogenesis to treatment concepts in humans. Mol Metab [Internet]. 2020;101122.

16. Leamy AK, Egnatchik RA, Young JD. Molecular mechanisms and the role of saturated fatty acids in the progression of non-alcoholic fatty liver disease. Prog Lipid Res [Internet]. 2013;52(1):165-74.
17. Marra F, Svegliati-Baroni G. Lipotoxicity and the gut-liver axis in NASH pathogenesis. J Hepatol [Internet]. 2018;68(2):280-95.
18. Pierantonelli I, Svegliati-Baroni G. Nonalcoholic Fatty Liver Disease: Basic Pathogenetic Mechanisms in the Progression from NAFLD to NASH. Transplantation. 2019;103(1):E1-13.
19. Schweiger M, Romauch M, Schreiber R, Grabner GF, Hütter S, Kotzbeck P, et al. Pharmacological inhibition of adipose triglyceride lipase corrects high-fat diet-induced insulin resistance and hepatosteatosis in mice. Nat Commun. 2017;8(May 2016).
20. Takahashi Y, Fukusato T. Histopathology of nonalcoholic fatty liver disease/nonalcoholic steatohepatitis. World J Gastroenterol. 2014;20(42):15539-48.
21. Gilissen J, Jouret F, Pirotte B, Hanson J. Insight into SUCNR1 (GPR91) structure and function. Pharmacol Ther [Internet]. 2016;159:56-65.
22. De Castro Fonseca M, Aguiar CJ, Da Rocha Franco JA, Gingold RN, Leite MF. GPR91: Expanding the frontiers of Krebs cycle intermediates. Cell Commun Signal [Internet]. 2016;14(1):1-9.
23. Li YH, Woo SH, Choi DH, Cho EH. Succinate causes α-SMA production through GPR91 activation in hepatic stellate cells. Biochem Biophys Res Commun [Internet]. 2015;463(4):853-8.
24. Jegatheesan P, De Bandt JP. Fructose and NAFLD: The multifaceted aspects of fructose metabolism. Nutrients. 2017;9(3):1-13.
25. van Diepen JA, Robben JH, Hooiveld GJ, Carmone C, Alsady M, Boutens L, et al. SUCNR1-mediated chemotaxis of macrophages aggravates obesity-induced inflammation and diabetes. Diabetologia. 2017;60(7):1304-13.
26. Peruzzotti-Jametti L, Bernstock JD, Vicario N, Costa ASH, Kwok CK, Leonardi T, et al. Macrophage-Derived Extracellular Succinate Licenses Neural Stem Cells to Suppress Chronic Neuroinflammation. Cell Stem Cell. 2018;22(3):355-368.e13.
27. Zhou J, Zhou F, Wang W, Zhang XJ, Ji YX, Zhang P, et al. Epidemiological Features of NAFLD From 1999 to 2018 in China. Hepatology. 2020;71(5):1851-64.
28. Schuster S, Cabrera D, Arrese M, Feldstein AE. Triggering and resolution of inflammation in NASH. Nat Rev Gastroenterol Hepatol [Internet]. 2018;15(6):349-64.
29. Mehcanobiology Institute 2018. National University of Singapore. What is the NF-κB pathway? Available at: https://www.mechanobio.info/what-is-mechanosignaling/signaling-pathways/what-is-the-nf-%CE%BAb-pathway/#what-is-the-nf-%ce%bab-pathway
30. Wellen KE, Hotamisligil GS. Inflammation, stress, and diabetes. J Clin Invest. 2005;115(5):1111-9.
31. Luo JL, Kamata H, Karin M. IKK/NF-κB signaling: Balancing life and death - A new approach to cancer therapy. J Clin Invest. 2005;115(10):2625-32.

32. Karin M, Delhase M. The IκB kinase (IKK) and NF-κB: Key elements of proinflammatory signalling. Semin Immunol. 2000;12(1):85-98.
33. Abcam.com. Overview of NF-κB pathway. Available at: https://www.abcam.com/research-areas/overview-of-nf-kb-signaling#nf-kb-pathways
34. Banerjee S, Biehl A, Gadina M, Hasni S, Schwartz DM. JAK–STAT Signaling as a Target for Inflammatory and Autoimmune Diseases: Current and Future Prospects. Drugs. 2017;77(5):521-46.
35. Schindler C, Plumlee C. Inteferons pen the JAK-STAT pathway. Semin Cell Dev Biol. 2008;19(4):311-8.
36. Haan C, Rolvering C, Raulf F, Kapp M, Drückes P, Thoma G, et al. Jak1 has a dominant role over Jak3 in signal transduction through γc-containing cytokine receptors. Chem Biol. 2011;18(3):314-23.
37. Lomonaco R, Ortiz-Lopez C, Orsak B, Webb A, Hardies J, Darland C, et al. Effect of adipose tissue insulin resistance on metabolic parameters and liver histology in obese patients with nonalcoholic fatty liver disease. Hepatology. 2012;55(5):1389-97.
38. Lebeaupin C, Vallée D, Hazari Y, Hetz C, Chevet E, Bailly-Maitre B. Endoplasmic reticulum stress signalling and the pathogenesis of non-alcoholic fatty liver disease. J Hepatol [Internet]. 2018;69(4):927-47.
39. Walter P, Ron D. The unfolded protein response: From stress pathway to homeostatic regulation. Science (80-). 2011;334(6059):1081-6.
40. Mori K. Signaling pathways in the unfolded protein response: Development from yeast to mammals. J Biochem. 2009;146(6):743-50.
41. Jain BP. An Overview of Unfolded Protein Response Signaling and Its Role in Cancer. Cancer Biother Radiopharm. 2017;32(8):275-81.
42. Schindler AJ, Schekman R. In vitro reconstitution of ER-stress induced ATF6 transport in COPII vesicles. Proc Natl Acad Sci U S A. 2009;106(42):17775-80.
43. Harding HP, Zhang Y, Scheuner D, Chen JJ, Kaufman RJ, Ron D. Ppp1r15 gene knockout reveals an essential role for translation initiation factor 2 alpha (eIF2α) dephosphorylation in mammalian development. Proc Natl Acad Sci U S A. 2009;106(6):1832-7.
44. Song MJ, Malhi H. The unfolded protein response and hepatic lipid metabolism in non alcoholic fatty liver disease. Pharmacol Ther. 2019;203:107401. doi:10.1016/j.pharmthera.2019.107401
45. Khambu B, Yan S, Huda N, Liu G, Yin XM. Autophagy in non-alcoholic fatty liver disease and alcoholic liver disease. Liver Res [Internet]. 2018;2(3):112-9.
46. Tanaka S, Hikita H, Tatsumi T, et al. Rubicon inhibits autophagy and accelerates hepatocyte apoptosis and lipid accumulation in nonalcoholic fatty liver disease in mice. Hepatology. 2016;64(6):1994-2014.

47. Cho C, Park H, Ho A, Semple IA, Kim B, Park H, et al. Lipotoxicity induces hepatic protein inclusions through TBK1- mediated p62/SQSTM1 phosphorylation Chun-Seok. Hepatology. 2018;68(4):1331-46.
48. Allaire M, Rautou PE, Codogno P, Lotersztajn S. Autophagy in liver diseases: Time for translation? J Hepatol [Internet]. 2019;70(5):985-98.
49. Khaminets A, Behl C, Dikic I. Ubiquitin-Dependent And Independent Signals In Selective Autophagy. Trends Cell Biol [Internet]. 2016;26(1):6-16.
50. Sahu R, Kaushik S, Clement CC, Cannizzo ES, Scharf B, Follenzi A, et al. Microautophagy of Cytosolic Proteins by Late Endosomes. Dev Cell [Internet]. 2011;20(1):131-9.
51. Schneider JL, Cuervo AM. Liver autophagy: Much more than just taking out the trash. Nat Rev Gastroenterol Hepatol. 2014;11(3):187-200.
52. Wang X, Zhang X, Chu ESH, Chen X, Kang W, Wu F, et al. Defective lysosomal clearance of autophagosomes and its clinical implications in nonalcoholic steatohepatitis. FASEB J. 2018;32(1):37-51.
53. Younossi ZM, Koenig AB, Abdelatif D, Fazel Y, Henry L, Wymer M. Global epidemiology of nonalcoholic fatty liver disease—Meta-analytic assessment of prevalence, incidence, and outcomes. Hepatology. 2016;64(1):73-84.
54. Roeb E, Geier A. Nichtalkoholische Steatohepatitis (NASH) aktuelle Behandlungsempfehlungen und zukünftige Entwicklungen. TT - Nonalcoholic steatohepatitis (NASH) - current treatment recommendations and future developments. Z Gastroenterol [Internet]. 2019;57(4):508-17.
55. Estes C, Anstee QM, Arias-Loste MT, Bantel H, Bellentani S, Caballeria J, et al. Modeling NAFLD disease burden in China, France, Germany, Italy, Japan, Spain, United Kingdom, and United States for the period 2016–2030. J Hepatol [Internet]. 2018;69(4):896-904.
56. Armstrong MJ, Gaunt P, Aithal GP, Barton D, Hull D, Parker R, et al. Liraglutide safety and efficacy in patients with non-alcoholic steatohepatitis (LEAN): A multicentre, double-blind, randomised, placebo-controlled phase 2 study. Lancet. 2016;387(10019):679-90.
57. Marchesini G, Day CP, Dufour JF, Canbay A, Nobili V, Ratziu V, et al. EASL-EASD-EASO Clinical Practice Guidelines for the management of non-alcoholic fatty liver disease. J Hepatol [Internet]. 2016;64(6):1388-402.
58. Sundström L, Greasley PJ, Engberg S, Wallander M, Ryberg E. Succinate receptor GPR91, a Gαi coupled receptor that increases intracellular calcium concentrations through PLCβ. FEBS Lett. 2013;587(15):2399-404.
59. Mills EL, Pierce KA, Jedrychowski MP, Garrity R, Winther S, Vidoni S, et al.. Accumulation of succinate controls activation of adipose tissue thermogenesis. Nature. 2018 Aug;560(7716):102-106.
60. Henquin JC. The dual control of insulin secretion by glucose involves triggering and amplifying pathways in β-cells. Diabetes Res Clin Pract [Internet]. 2011;93(SUPPL. 1):S27-31.

61. Maurice J, Manousou P. Non-alcoholic fatty liver disease. Clin Med (Lond). 2018 Jun;18(3):245-250.
62. Jesse M. C et al. Hepatic Fibrosis – Hepatic and Biliary Disorders. MSD Manual Professional Version, MSD Manuals. 2019; 12. Available at: <https://www.msdmanuals.com/professional/hepatic-and-biliary-disorders/fibrosis-and-cirrhosis/hepatic-fibrosis >
63. Crossan C, Majumdar A, Srivastava A, Thorburn D, Rosenberg W, Pinzani M, et al. Referral pathways for patients with NAFLD based on non-invasive fibrosis tests: Diagnostic accuracy and cost analysis. Liver Int. 2019;39(11):2052-60.
64. Friedman SL. Hepatic fibrosis-Overview. Toxicology. 2008;254(3):120-9.
65. Smigiel KS, Parks WC. Macrophages, Wound Healing, and Fibrosis: Recent Insights. Current Rheumatology Reports. 2018 Mar;20(4):17.
66. Nguyen G, Park SY, Le CT, Park WS, Choi DH, Cho EH. Metformin ameliorates activation of hepatic stellate cells and hepatic fibrosis by succinate and GPR91 inhibition. Biochem Biophys Res Commun [Internet]. 2018;495(4):2649-56.
67. Foglia B, Cannito S, Bocca C, Parola M, Novo E. ERK pathway in activated, myofibroblast-like, hepatic stellate cells: A critical signaling crossroad sustaining liver fibrosis. Int J Mol Sci. 2019;20(11).
68. Byrne CD, Targher G. NAFLD: A multisystem disease. J Hepatol [Internet]. 2015;62(S1):S47-64.
69. Dangana EO, Michael OS, Omolekulo TE, Areola ED, Olatunji LA. Enhanced hepatic glycogen synthesis and suppressed adenosine deaminase activity by lithium attenuates hepatic triglyceride accumulation in nicotine-exposed rats. Biomed Pharmacother [Internet]. 2019;109(July 2018):1417-27.
70. Henkel AS. Unfolded Protein Response Sensors in Hepatic Lipid Metabolism and Nonalcoholic Fatty Liver Disease. Semin Liver Dis. 2018;38(4):320-32.
71. Fujii T, Fujita N, Suzuki S, Tsuji T, Takaki T, Umezawa K, et al. The unfolded protein response mediated by PERK is casually related to the pathogenesis of intervertebral disc degeneration. J Orthop Res. 2018;36(5):1334-45.
72. Zhang Q, Zhao K, Shen Q, Han Y, Gu Y, Li X, et al. HHS Public Access. 2016;525(7569):389-93.
73. McCreath KJ, Espada S, Gálvez BG, Benito M, de Molina A, Sepúlveda P, Cervera AM. Targeted disruption of the SUCNR1 metabolic receptor leads to dichotomous effects on obesity. Diabetes. 2015;64(4):1154-67.
74. Tan Q, Hu J, Yu X, Guan W, Lu H, Yu Y, Yu Y, Zang G, Tang Z. The Role of IL-1 Family Members and Kupffer Cells in Liver Regeneration. Biomed Res Int. 2016;2016:6495793.
75. Paglialunga S, Dehn CA. Clinical assessment of hepatic de novo lipogenesis in non-alcoholic fatty liver disease. Lipids Health Dis [Internet]. 2016;15(1):1-10.

76. Gan L, Xiang W, Xie B, Yu L. Molecular mechanisms of fatty liver in obesity. Front Med. 2015;9(3):275-87.
77. Lambert JE, Ramos-Roman MA, Browning JD, Parks EJ. Increased de novo lipogenesis is a distinct characteristic of individuals with nonalcoholic fatty liver disease. Gastroenterology. 2014;146(3):726-35.
78. Adjibade P, St-sauveur VG, Bergeman J, Huot M, Khandjian EW, Mazroui R. DDX3 regulates endoplasmic expression. 2017;(October):1-12.
79. González-Rodríguez A, Mayoral R, Agra N, Valdecantos MP, Pardo V, Miquilena-Colina ME, et al. Impaired autophagic flux is associated with increased endoplasmic reticulum stress during the development of NAFLD. Cell Death Dis. 2014;5(4).
80. Lei Y, Wang S, Ren B, Wang J, Chen J, Lu J, et al. CHOP favors endoplasmic reticulum stress-induced apoptosis in hepatocellular carcinoma cells via inhibition of autophagy. PLoS ONE 2017;12(8): e0183680.
81. Mao L, Kitani A, Strober W, Fuss IJ. The role of NLRP3 and IL-1β in the pathogenesis of inflammatory bowel disease. Front Immunol. 2018;9(NOV):1-9.

Supplementary material

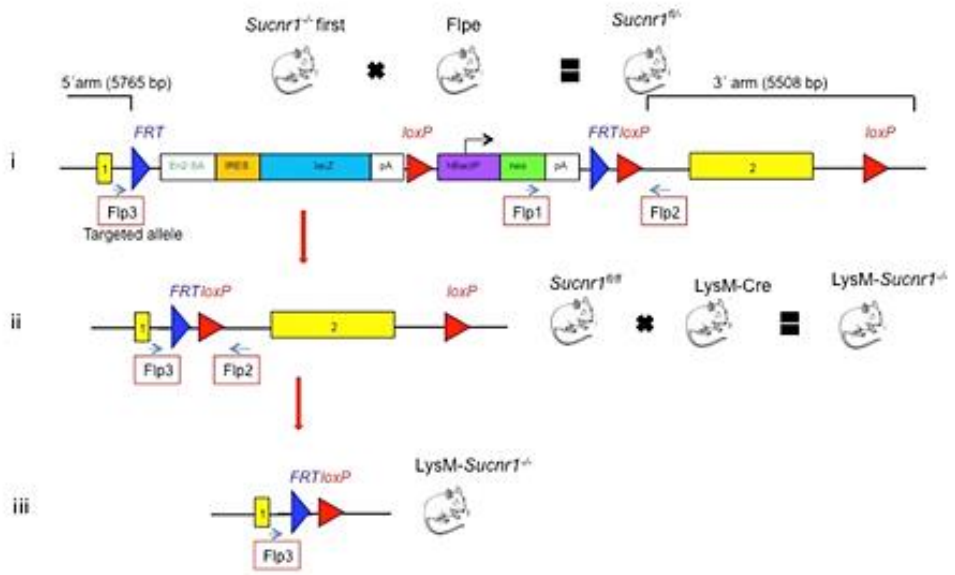

Fig. 1. Generation of myeloid cell-specific *Sucnr1* KO mice. (i) Schematic representation of the targeting vector structure: *Sucnr1* locus with the loxP sites (red arrowheads) located on both sides of exon 2 (yellor box). (ii) *Sucnr1* locus after being subjected to Flp-mediated recombination of the FRT sites (blue arrowheads). (iii) Through Cre-mediated deletion of loxP sites resulting mice are myeloid cell-specific *Sucnr1* KO. Primers used for genotyping are represented by small arrows: flp2 and flp3. Adapted from Keiran N et al. *SUCNR1 controls an anti-inflammatory program in macrophages to regulate the metabolic response to obesity.* Nat Immunol. 2019.

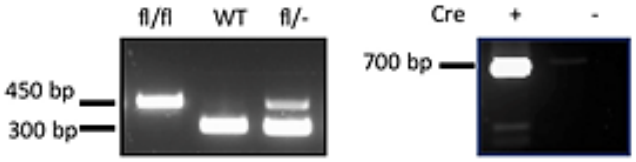

Fig. 2. Systematic mice genotyping. On the right, a representative image of systematical mice genotyping. As a result, a 300 bp band can be identified for the wild-type (WT) allele and a 450 bp band can be identified for alleles that contain loxP sites (fl/fl). On the left, a 700 bp band is shown corresponding to presence of the Cre-recombinase gene in mice. Adapted from Keiran N et al. *SUCNR1 controls an anti-inflammatory program in macrophages to regulate the metabolic response to obesity.* Nat Immunol. 2019.

Table 1. Description of Rodent Diet content. Choline-deficient high fat diet, with a 45% of kcal consisting of fat. Reference #D05010402 from Research Diets. Formulated by E.A. Ulman, Ph.D., Research Diets, Inc., 8/26/98, and 3/11/99. See Van Heek et al., J. Clin. Invest. 99:385-390, 1997.

Product #	D05010402	
	gm%	*kcal%*
Protein	23.7	*20.0*
Carbohydrate	41.5	*35.1*
Fat	23.7	*44.9*
Total		*100.0*
kcal/gm	**4.74**	
Ingredient	**gm**	*kcal*
Casein, 80 Mesh	200	*800*
L-Cystine	3	*12*
Corn Starch	72.8	*291.2*
Maltodextrin 10	100	*400*
Sucrose	172.8	*691.2*
Cellulose, BW200	50	*0*
Soybean Oil	25	*225*
Lard	177.5	*1597.5*
Mineral Mix, S10026	10	*0*
DiCalcium Phosphate	13	*0*
Calcium Carbonate	5.5	*0*
Potassium Citrate, 1 H2O	16.5	*0*
Vitamin Mix, V10001	10	*40*
Choline Bitartrate	0	*0*
FD&C Yellow Dye #5	0	*0*
FD&C Red Dye #40	0.025	*0*
FD&C Blue Dye #1	0.025	*0*
Total	**856.15**	***4057***

Table 2. TaqMan™ probes used for relative gene expression analysis through RT-PCR.

Gene	TaqMan™ probe
Housekeeping gene	
Eukaryotic 18S ribosomal RNA	Mm01268569_m1
Markers of lipid metabolism	
ACC	Mm01304257_m1
FAS	Mm00662319_m1
SREBP1c	Mm00550338_m1
PPARγ	Mm00440940_m1
HSL	Mm01240677_m1

ATGL	Mm00503040_m1
CPT1α	Mm01231183_m1
Markers of glycogen metabolism	
GYS-2	Mm01267381_g1
PYGL	Mm01289790_m1
PEPCK	Mm01247058_m1
Inflammatory markers	
IL-1β	Mm00434228_m1
IL-6	Mm00446190_m1
IL-12β	Mm01288989_m1
TNFα	Mm00443258_m1
Browning markers	
UCP1	Mm01244861_m1

ACC: Acetyl-CoA Carboxylase, FAS: Fatty Acid Synthase, SREBP1c: Sterol regulatory element-binding protein, PPARγ: Peroxisome proliferator-activated receptor gamma, HSL: Hormone-sensitive lipase, ATGL: Adipose triglyceride lipase, CPT1α: Carnitine palmitoyl-transferase I alpha, GYS-2: Glycogen synthase 2, PYGL: Liver form of glycogen phosphorylase, PEPCK: Phosphoenolpyruvate carboxykinase, IL-1β: Interleukin 1 beta, IL-6: Interleukin 6, IL-12β: Interleukin 12 beta, TNFα: Tumor necrosis factor alpha, UCP1: Uncoupling protein 1.